โครงการ

การเรียนการสอนเพื่อเสริมประสบการณ์

ชื่อโครงการ การศึกษาการดูดซับโมเลกุลขนาดเล็ก บนพื้นผิวของกราฟีนและกราฟีนที่ถูกเจือ
Study of small molecular adsorption on doped and non-doped Graphenes

ชื่อนิสิต นายฐิติพงศ์ สิทธิ์ธนพุฒิกร เลขประจำตัว 5933027723
ภาควิชา เคมี

ปีการศึกษา 2562

คณะวิทยาศาสตร์ จุฬาลงกรณ์มหาวิทยาลัย

การศึกษาการดูดซับโมเลกุลขนาดเล็ก บนพื้นผิวของกราฟีนและกราฟีนที่ถูกเจือ

โดย
นายฐิติพงศ์ สิทธิ์ธนพุฒิกร

รายงานนี้เป็นส่วนหนึ่งของการศึกษาตามหลักสูตร
ปริญญาวิทยาศาสตรบัณฑิต
ภาควิชาเคมี คณะวิทยาศาสตร์
จุฬาลงกรณ์มหาวิทยาลัย
ปีการศึกษา 2562

Study of small molecular adsorption on doped and non-doped graphenes

Mr. Thitipong Sitthanaputtikorn

In Partial Fulfilment for the Degree of Bachelor of Science

Department of Chemistry, Faculty of Science

Chulalongkorn University

Academic Year 2019

Project Title	Study of small molecular adsorption on doped and non-doped graphene
By	Mr. Thitipong Sitthanaputtikorn
Field of study	Chemistry
Project Advisor	Professor Vithaya Ruangpornvisuti, Dr.rer.nat.

Accepted by the Department of Chemistry, Faculty of Science, Chulalongkorn University in Partial Fulfillment of the Requirements for the Degree of Bachelor for Science.

PROJECT COMMITTEE

1. Associate Professor Viwat	Vchirawongkwin, Dr.rer.nat.	Chair Committee
2. Associate Professor Fuangfa	Unob, Ph.D.	Committee
3. Professor Vithaya	Ruangpornvisuti, Dr.rer.nat.	Project Advisor

This project has been endorsed by Head of Department of Chemistry

(Professor Vithaya Ruangpornvisuti, Dr.rer.nat)
Project Advisor

(Associate Professor Vudhichai Parasuk, Ph.D.)
Head of Department of Chemistry
10 / June / 2020

โครงการ การศึกษาการดูดซับโมเลกุลขนาดเล็ก บนพื้นผิวของกราฟีนและกราฟีนที่ถูกเจือ
ชื่อนิสิตในโครงการ นายฐิติพงศ์ สิทธิ์ธนพุฒิกร เลขประจำตัว 5933027723
ชื่ออาจารย์ที่ปรึกษา ศาสตราจารย์ ดร.วิทยา เรืองพรวิสุทธิ์
ภาควิชาเคมี คณะวิทยาศาสตร์ จุฬาลงกรณ์มหาวิทยาลัย ปีการศึกษา 2562

บทคัดย่อ

โครงรูปที่เหมาะสมของการดูดซับโมเลกุลแก๊ส ได้แก่ ไฮโดรเจน น้ำ ไนโตรเจนไดออกไซด์ และคาร์บอนมอนอกไซด์ ที่ถูกดูดซับบนกราฟีน และกราฟีนที่ถูกเจือด้วยโลหะทรานซิชั่น ได้แก่ สแกนเดียม ไทเทเนียม เหล็ก โคบอลต์ นิกเกิล สังกะสี และทองคำ โดยใช้การคำนวณพีรีออดิก วิธีเอสซีซี-ดีเอฟทีบี ผลการคำนวณจะรายงานค่าพลังงานการดูดซับของแก๊ส ไฮโดรเจน น้ำ ไนโตรเจนไดออกไซด์ และคาร์บอนมอนอกไซด์ บนกราฟีนที่เจือด้วยโลหะทรานซิชั่นต่างกัน ค่าพลังงานการดูดซับที่ดีที่สุดสำหรับการดูดซับ ไฮโดรเจน น้ำ ไนโตรเจนไดออกไซด์ และ คาร์บอนมอนออกไซด์ คือ พื้นผิวกราฟีนที่ถูกเจือด้วย เหล็ก(ค่าพลังงานดูดซับ -66.85 กิโลแคลอรี่/โมล) ไทเทเนียม(ค่าพลังงานดูดซับ -62.17 กิโลแคลอรี่/โมล) โคบอลต์(ค่าพลังงานดูดซับ -126.67 กิโลแคลอรี่/โมล) และไทเทเนียม(ค่าพลังงานดูดซับ -52.09 กิโลแคลอรี่/โมล) ตามลำดับ กราฟีนที่ถูกเจือด้วยทองคำ สามารถนำไปเป็นวัสดุรับรู้แก๊สไฮโดรเจน และกราฟีนที่ถูกเจือด้วยเหล็กสามารถนำไปเป็นวัสดุรับรู้ น้ำ แก๊สไนโตรเจนไดออกไซด์ และคาร์บอนมอนออกไซด์ได้

คำสำคัญ: พลังงานการดูดซับ, แก๊ส ไฮโดรเจน น้ำ ไนโตรเจนไดออกไซด์ และ คาร์บอนมอนออกไซด์, อนุพันธ์ของกราฟีนเจือด้วยโลหะ, ดีเอฟทีบี

Project Title Study of small molecular adsorption on doped and non-doped graphene
Student Name Mr. Thitipong Sitthanaputtikorn Student ID 5933027723
Advisor Name Professor Vithaya Ruangpornvisuti, Dr.rer.nat.
Department of Chemistry, Faculty of Science, Chulalongkorn University, Academic Year 2019

Abstract

The structure optimizations of all configuration of gases H_2, H_2O, N_2O and CO molecules adsorbed on graphene and its doping derivatives with transition metals (Sc, Ti, Fe, Co, Ni, Zn and Au) were carried out using self-consistent charge density functional tight-binding (SCC-DFTB) periodic calculations. Adsorption energies of gases H_2, H_2O, N_2O and CO on doping derivatives of graphene with different transition metal atoms (ScG, TiG, FeG, CoG, NiG, ZnG and AuG) were obtained and reported. The strongest adsorption of H_2, H_2O, N_2O and CO are found on FeG (ΔE_{ads} =-66.85 kcal/mol), TiG (ΔE_{ads} =-62.17 kcal/mol), CoG (ΔE_{ads} =-126.67 kcal/mol) and TiG (ΔE_{ads} =-52.09 kcal/mol) surfaces, respectively. AuG is suggested as the hydrogen gas sensor. FeG is suggested as the water, nitrogen dioxide, carbon monoxide gas sensor.

Keywords: Adsorption energies; gases H_2, H_2O, N_2O and CO; metal doped graphene derivatives; DFTB

ACKNOWLEDGEMENTS

This study was carried out at the Department of Chemistry, Faculty of Science, Chulalongkorn University. I would like to express my sincere thank to my advisor Professor Dr. Vithaya Ruangpornvisuti for his useful guidance, encourangement, understanding and constant support throughout the course of this research. I was so appreciated with his opportunity that provided me to be able to join the study under his instruction with kindness and valuable guidance.

I would like to really thank Associate Professor Dr.Viwat Vchirawongkwin and Associate Professor Dr.Fuangfa Unob for kindly serving on my committee. Their sincere suggestions are definitely imperative for accomplishing my project.

Special thanks to my seniors in VR lab (Supramolecular Chemistry Research Unit) who encouraged and gave me tips to get the work successful. I also would like to thank all teaching staff and my friends for all their good suggestions, friendship and continuous encouragement.

Finally, I would like to thank my parents and my grandmother who are important in my life. Thank you for always supporting and trusting in my decisions. They always love me and I am very proud to be a part of my family.

Mr. Thitipong Sitthanaputtikorn

CONTENTS

Page

LIST OF FIGURES

Page

LIST OF TABLES

Page

CHAPTER I

INTRODUCTION

1.1 Background and Literature review

The surface graphene of transition metals doped on adsorptions of H_2 [1], H_2O [1], CO [1] and N_2O [2]. Graphene doped with transition metal and heteroatoms has been reported as a useful method to tailor the physical and chemical properties of graphene, demonstrating that graphene doping improves the interaction with several molecules [3]. The doping of graphene with transition metals have been investigated by analyzing the geometric structure, adsorption energy, charge transfer, charge density, energy band, and density of states of each adsorption models [4]. As small gases adsorption on the graphene have been useful information for their adsorption abilities and reactions, the graphene of which the structure is a large surface area, superior mechanical flexibility, high chemical and thermal stability.

Density-functional tight-binding (DFTB) is a semi-empirical method which based on density-functional theory (DFT). DFTB is therefore an appropriate method for calculations in large system compound with the DFT method.

In the present work, small gas molecules (H_2, H_2O, N_2O, CO) adsorbed on graphene and its transition metals (Sc, Ti, Fe, Co, Ni, Zn and Au) doping derivatives have been investigated by DFTB method.

1.2 Theoretical background

Computational chemistry is one of the most branches of chemistry that widely used to investigate the molecular structure, molecular properties, reactions mechanisms and energies. There are two types of computational chemistry namely quantum mechanics (QM) and molecular mechanics (MM). Quantum mechanical method is categorized into semi-empirical, ab initio and density functional theory (DFT) methods. Quantum chemical calculation has been used to calculate structures, properties and interaction of molecules [5]. Density-functional tight-binding (DFTB), one of quantum mechanics method based on DFT was employed to calculate in the present work.

1.2.1 Semi-empirical method

Semi–empirical methods are based on the principle of quantum chemistry which derived from Hartree–Fock calculations by applying empirical corrections. The integrals are determined directly from experimental data. The advantage of semi–empirical calculations is reduced computation time, making them commonly used in the application for large molecules [6]. The methods in semi–empirical such as PM3, AM1 and MNDO are generally used for predicting various properties such as molecular structure, heats of formation, ionization potentials and electron affinities [7].

A semi-empirical can be introduced within the theoretical framework of DFT. The Self-Consistent Charge Density Functional Tight Binding (SCC-DFTB) theory is obtained by replacing the quantum mechanical electron density by atomic partial charges [8]. These semi-empirical DFT methods are computationally as efficient as other semi-empirical models and have during recent years also been extended to study, for example, optical and excited-state properties [9]. In contrast to other semi-empirical methods, DFTB is not based on fitting to experimental data but rather to DFT calculations. As for DFT and the other semi-empirical methods, SCC-DFTB has difficulties in describing dispersion forces, but inclusion of empirical dispersion corrections is found to improve agreement with experiments [10].

1.2.2 Density functional theory (DFT) method [11]

DFT has become widely the popular method for calculating properties of many–electron system. This methods are founded by the Hohenberg–Kohn (HK) theorems [12]. The HK theorems constructed the electronic density as variable to calculate electronic–structure and the energy of a molecule is come from the electron density replaced in a wave function. HK–DFT shows that electron density functional, $F(p_0)$, can define the ground state properties functional, $f(x)$, e.g. energy, E_0 of a many–electron system.

$$E_0 = F[\rho_0] = E[\rho_0] \tag{1.1}$$

The total electronic energy of molecule to obtain from a trial electron density, ρ_t, is the energy of the electrons in motion under the nuclear potential called external potential, $\upsilon(r)$. The energy functional of exact ground state electron density, E_v, was stated by the second HK–DFT.

$$E_v[\rho_t] \geq E[\rho_0] \tag{1.2}$$

where ρ_0 is exact ground state energy according to exact electronic density.

1.2.2.1 The KS Equations

The KS equations have theorem obtained from using the variation principle, which the second HK theorem convinces applies to DFT. We use the fact that the electron density of the reference system, which is the same as that of our real system, is given by

$$\rho_0 = \rho_r = \sum_{i=1}^{2n} \left| \psi_i^{KS}(1) \right|^2 \tag{1.3}$$

where the ψ_i^{KS} are the KS spatial orbital. Replacing the above definition for the orbitals to the energy and fluctuating E_0 with consideration to the point to the limitation that these remain orthonormal lead to the KS equations, algorithm is like to that used in deriving the HF equations,

$$\left[-\frac{1}{2}\nabla_i^2 - \sum_{nucleiA} \frac{Z_A}{\mathbf{r}_{1A}} + \int \frac{\rho(\mathbf{r}_2)}{r_{12}} d\mathbf{r}_2 + v_{XC}(1) \right] \psi_i^{KS}(1) = \varepsilon_i^{KS} \psi_i^{KS}(1) \tag{1.4}$$

where ε_i^{KS} are the KS energy levels and $v_{\mathrm{xc}}(1)$ is the exchange–correlation potential, arbitrarily determined here for electron number (1), because the KS equations have a fix of one electron equations with where subscript *i* operate over all the 2*n* electron in the system from 1 to *n*,. The exchange–correlation energy is determined as the functional derivative from $\rho(\mathrm{r})$

$$v_{\mathrm{xc}}(\mathrm{r}) = \frac{\delta E_{\mathrm{xc}}[\rho(\mathrm{r})]}{\delta \rho(\mathrm{r})} \tag{1.5}$$

We require the derivative v_{xc} for the KS equations, and the exchange–correlation functional itself for the energy equation. The following KS equations can be written as

$$\hat{h}^{KS}(1)\psi_i^{KS}(1) = \varepsilon_i^{KS}\psi_i^{KS}(1) \quad (1.6)$$

The KS operator $\hat{h}^{KS}$ is determined by equation (1.6). The difference between DFT method is the selection of the functional from of the exchange–correlation energy. Functional of DFT forms are often created to obtain a confident restricting behavior, and fitting parameters to understand correct data. Which functional is the better will have to be solved by comparing the efficiency with experiments or high–level wave mechanics calculations.

1.2.3 Density functional tight–binding (DFTB) method [12]

Density functional tight–binding (DFTB) method, one of quantum mechanics method based on DFT was used to calculate molecular and material properties, which has an efficient and fast quantum mechanical simulation method. DFTB can be derived from a Taylor expansion of the KS–DFT density functional

$$\rho(r) = \rho^0(r) + \delta\rho(r) \quad (1.7)$$

The exchange–correlation energy functional is described in a Taylor series and the total energy can be written as

$$E^{DFTB3}[\rho+\delta\rho] = E^0[\rho_0] + E^1[\rho_0,\delta\rho] + E^2[\rho_0,(\delta\rho)^2] + E^3[\rho_0,(\delta\rho)^3] \quad (1.8)$$

1.2.3.1 DFTB1

DFTB1 or non–self–consistent DFTB (non–SCC) DFTB is involved only the two terms of equation (1.8), $E^0[\rho_0]$ and $E^1[\rho_0, \delta\rho]$. DFTB1 is based on linear combination of atomic orbital (LCAO) of the KS orbitals.

$$\varphi_i = \sum_\mu c_{\mu i}\varphi_\mu \quad (1.9)$$

The atomic orbitals (AOs) are received from DFT calculations of the corresponding atoms.

$$|\phi_\mu\rangle = |\phi_\mu\rangle - \Sigma_{b\neq a}\Sigma_\kappa|\phi_\kappa^b\rangle\langle\phi_\kappa^b|\phi_\mu\rangle,\ \mu\varepsilon\{a\} \quad (1.10)$$

where $|\phi_\mu\rangle$ is the valences AO μ at atom *a* and $|\phi_\kappa^b\rangle$ is a core orbital at atom *b*, as obtained from the corresponding atomic calculations.

The atomic KS equations are usually solved applying an additional potential to the atomic KS equations.

$$\left[-\frac{1}{2}\Delta^2 + v^{\text{eff}}\left[\rho^{\text{atom}}\right] + \left(\frac{r}{r_0}\right)^2\right]\phi_\mu = \varepsilon_\mu \phi_\mu \tag{1.11}$$

Then, with AO basis and initial density determined, the KS equation can be solved leading to the energy.

$$E^1 = \sum_i n_i \varepsilon_I \tag{1.12}$$

where n_I is an occupation number of KS orbital *i*.

This is the electronic energy of the DFTB method. To find the total energy, the E_0 is to be approximated. This term in DFTB is approximated by a sum of pair potentials called repulsive energy term.

$$E_0\left[\rho_0\right] \approx E_{\text{rep}} = \frac{1}{2}\sum_{ab} v_{ab}^{\text{rep}} \tag{1.13}$$

The total energy for DFTB1 is defined as

$$E^{\text{DFTB1}} = \sum_i n_i \varepsilon_i + \frac{1}{2}\sum_{ab} v_{ab}^{\text{rep}} \tag{1.14}$$

1.2.3.2 DFTB2

DFTB2 approximates E^2 term in equation (1.8) further. The density fluctuations are written as a superposition of atomic contributions.

$$\Delta\rho = \sum_a \delta\rho_a \tag{1.15}$$

By assessed assuming an exponentially decaying charge density

$$\Delta\rho \approx \Delta q_a \frac{\tau_a^3}{8\pi} e^{-\tau_a |r - R_0|} \tag{1.16}$$

E^2 in (1.8) is defined as

$$E^2\left(\tau_a,\tau_b,R_{ab}\right)=\frac{1}{2}\sum_{ab}\Delta q_a\Delta q_b\gamma_{ab}\left(\tau_q,\tau_b,R_{ab}\right) \tag{1.17}$$

The Hartree term therefore explains the interaction of the charge density fluctuations $\delta\rho a$ and $\delta\rho b$, which decreases to Coulomb interaction of partial charges Δqa and Δqb for large distances, i.e. γab approaches $1/Rab$ for huge distances.

1.2.3.3 DFTB3

For E^3 , the same approximations are started as for E^2. The third–order terms explain the change of the chemical hardness of an atom with its charge state, a new parameter is introduced, the chemical hardness derivative. A function Γ_{ab} results as derivative of the γ–function with point to charge by introducing the Hubbard derivative parameter.

With all these approximations, the SCC–DFTB total energy in the third order is given by

$$E^{\mathrm{DFTB3}} = \Sigma_{iab}\Sigma_{\mu\in a}\Sigma_{\nu\in b}\, n_i c_{\mu i} H^0_{\mu\nu} + \frac{1}{2}\sum_{ab}\Delta q_a\Delta q_b\gamma^h_{ab} + \frac{1}{3}\sum_{ab}q^2_a\Delta q_b\Gamma_{ab} + \frac{1}{2}\sum_{ab}\Delta V_{ab}^{rep} \tag{1.18}$$

1.3 Objectives

In this study, the adsorption energies, thermodynamic properties and charge transfer of gases H_2, H_2O, N_2O and CO adsorbed on transition metals (Sc, Ti, Fe, Co, Ni, Zn and Au) doped graphene derivatives compared with pristine graphene have been assessed using the periodic SCC-DFTB method.

CHAPTER II

COMPUTATIONAL DETAILS

2.1 Structure optimization

Full optimizations of adsorption structures of all configuration of gases H_2, H_2O, N_2O and CO molecules adsorbed on transition metals (Sc, Ti, Fe, Co, Ni, Zn and Au) doped and non-doped graphenes were carried out using self-consistent charge density functional tight-binding (SCC-DFTB) periodic calculations. All SCC-DFTB calculations were performed with the code of DFTB+ version 1.3 [13]. Parameter sets "mio-1-1" for H, C atoms . All SCC-DFTB calculations, the SCC tolerance were smaller than 1.0×10^{-6} e.

2.2 Adsorption of small gas on surface transition doped and non-doped graphene

The adsorption energies (ΔE_{ads}) for small gas adsorbed on the surface doped and non-doped graphene have been obtained using Equation (2.1).

$$\Delta E_{ads}\,(\text{gas}) = E(\text{gas/graphene}) - [E(\text{graphene}) + E(\text{gas})] \qquad (2.1)$$

where E(gas/graphene) is total energy of gas adsorbed on surface of G or MG (ScG, TiG, FeG, CoG, NiG, ZnG or AuG). E(gas) and E(graphene) are total energies of isolated gas and on surface of G or MG, respectively.

2.3 Percentage of energy–gap change compared with clean MG

Response: Sensor response represents the change in energy-gap of the gas sensor with respect to the initial energy gap of the graphene when exposed to various gases.

$$\Delta E\text{g} = [\frac{E\text{g(gas)} - E\text{g(ini)}}{E\text{g(ini)}}] \times 100$$

Where Eg(ini) is initial energy-gap of G or MG (ScG, TiG, FeG, CoG, NiG, ZnG or AuG) in ambient gas. Eg(gas) is energy-gap of the sensor in the presence of adsorption gas .

CHAPTER Ill

RESULTS AND DISCUSSION

3.1 The optimized structures of doped and non-doped graphene

The full optimization of graphene - in gas phase and periodic parameters x and y with fixed z dimension at 30.000 Å, computed by periodic the SCC-DFTB method were carried out and periodic parameters x = 19.8125 Å, y = 21.4576 Å were obtained by energy minimization with respect to parameters x and y. Optimized structures of pristine, Sc-, Ti-, Fe-, Co-, Ni-, Zn- and Au-doped G are shown in Figure 3.1.

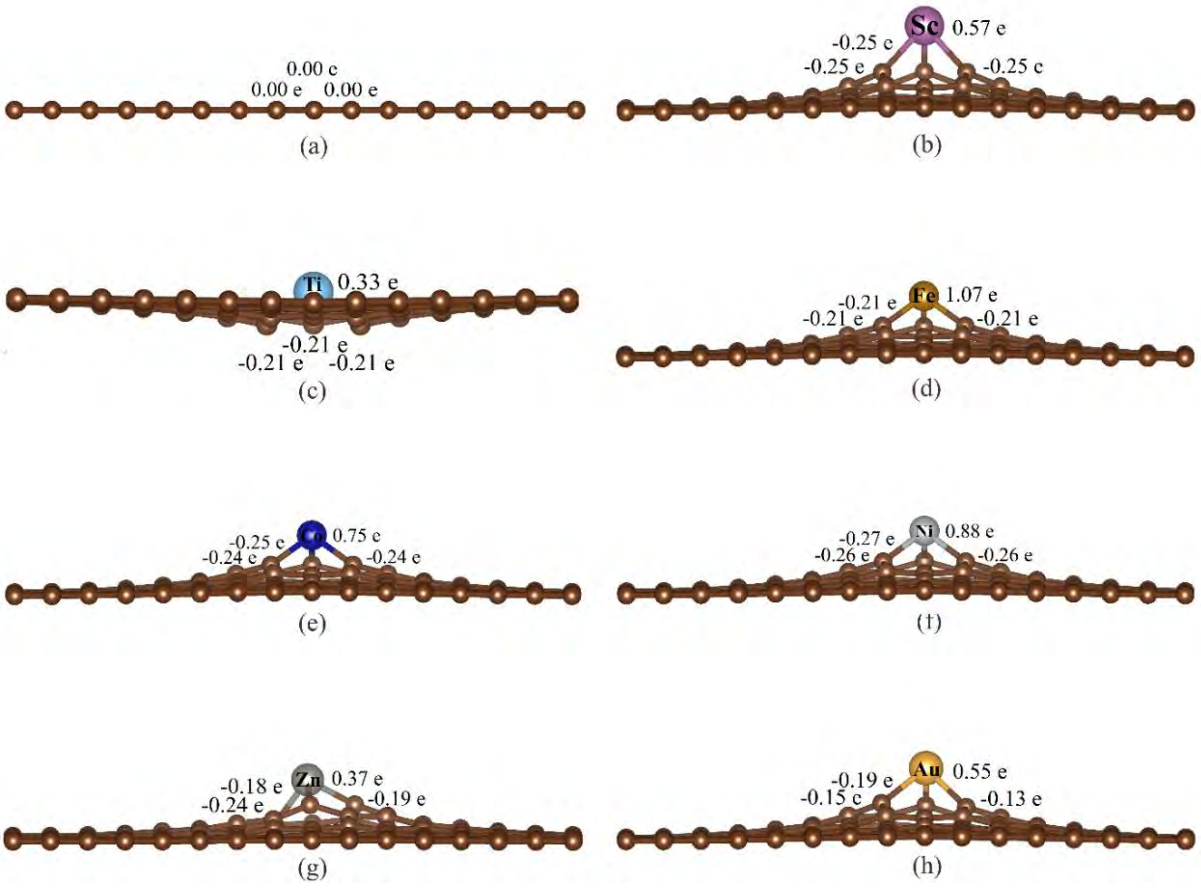

Figure 3.1 Optimized structures of (a) pristine, (b) Sc-doped G, (c) Ti-doped G, (d) Fe-doped G, (e) Co-doped G, (f) Ni-doped G, (g) Zn-doped G and (h) Au-doped G. Mülliken charges of selected atoms are labelled.

3.2 The optimized structures of metal doped and non-doped graphenes with H_2

The SCC-DFTB-optimized structures of H_2 adsorbed on the transition metal doped graphene derivatives, Sc-, Ti-, Fe-, Co-, Ni-, Zn- and Au-doped G are shown in Figure 3.2. It shows that H_2 adsorbed on G, ScG, TiG and ZnG are physical adsorption and on FeG, CoG, NiG and AuG are dissociative chemisorption. Adsorption abilities on H_2 of metal doped graphene derivatives are in order: FeG > AuG > CoG > NiG > TiG > ScG > ZnG > G.

Adsorption energies of the SCC-DFTB-optimized structure of H_2 adsorbed on the transition metal doped graphene derivatives compared with graphene and energy gaps of their adsorption structures and energy–gap changes (in %) compared with clean MG, are shown in Table 3.1. As AuG is able to strongly adsorb hydrogen molecule with high energy–gap change (ΔE_g =65.71%), the AuG can therefore be performed as hydrogen gas sensor.

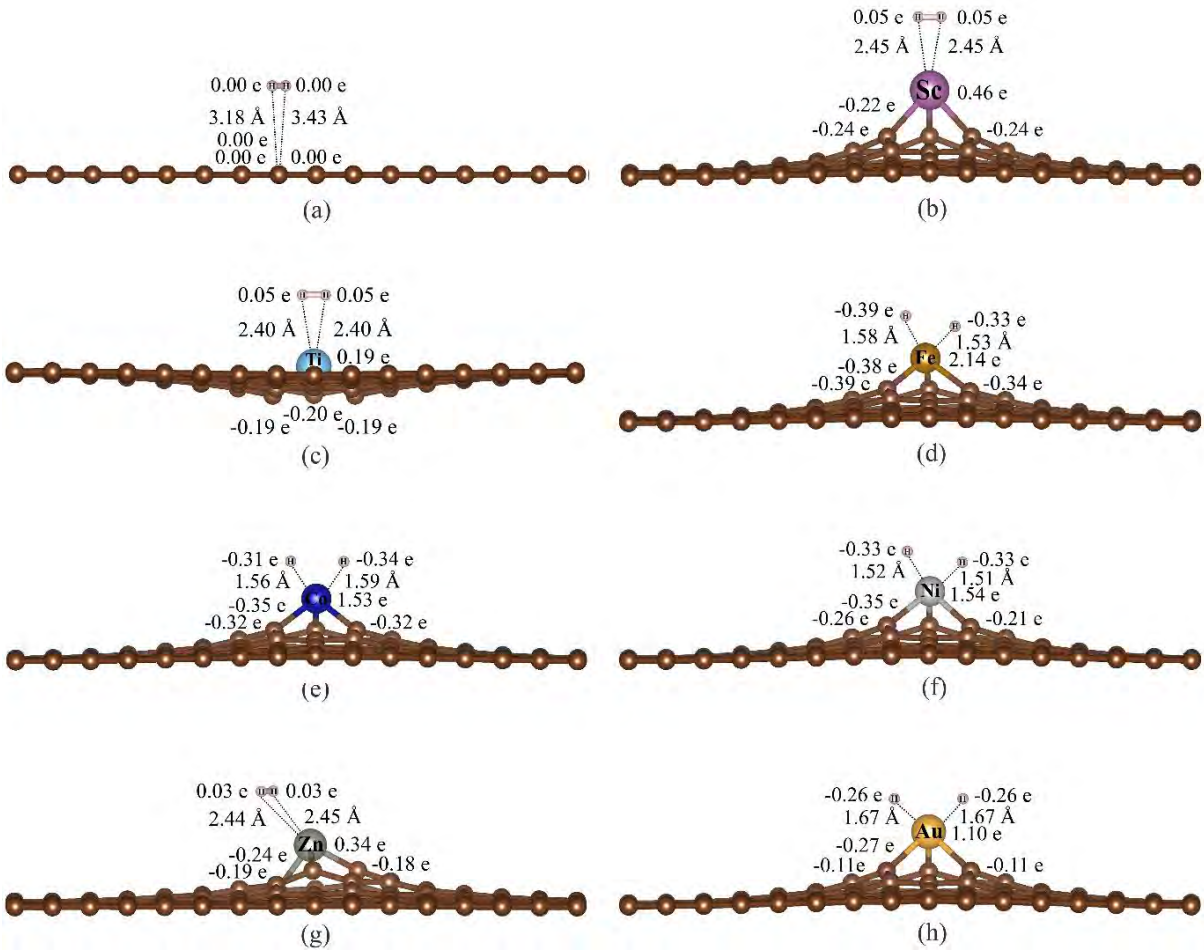

Figure 3.2 Adsorption of hydrogen molecule on (a) pristine, (b) Sc-doped G, (c) Ti-doped G, (d) Fe-doped G, (e) Co-doped G, (f) Ni-doped G, (g) Zn-doped G and (h) Au-doped G. Mülliken charges of related atoms and bond distances between hydrogen molecule and doped atom are shown.

Table 3.1 Adsorption energies of H_2 adsorbed on the transition metal doped graphene derivatives compared with graphene and energy gaps of their adsorption structures and energy–gap change in percentage compared with clean MG, computed by the SCC-DFTB method.

Adsorption	ΔE_{ads}[a]	E_g[b]	ΔE_g[c]
G	-	1.71	-
$H_2 + G \rightarrow H_2/G$	-1.73	1.71	0.00
Sc-G	-	0.87	-
H_2 + Sc-G → H_2/Sc-G	-6.74	0.86	-1.15
Ti-G	-	0.89	-
H_2 + Ti-G → H_2/Ti-G	-11.16	0.88	-1.12
Fe-G	-	0.21	-
H_2 + Fe-G → H_2/Fe-G	-66.85	0.25	19.05
Co-G	-	0.54	-
H_2 + Co-G → H_2/Co-G	-29.02	0.65	20.37
Ni-G	-	0.62	-
H_2 + Ni-G → H_2/Ni-G	-16.32	0.84	35.48
Zn-G	-	0.66	-
H_2 + Zn-G → H_2/Zn-G	-4.66	0.68	3.03
Au-G	-	0.35	-
H_2 + Au-G → H_2/Au-G	-59.03	0.58	65.71

[a] At 298.15 K, in kcal/mol.

[b] In eV.

[c] Percentage of energy–gap change compared with clean MG.

Mülliken charges of related atoms of clean and H_2 molecule adsorbed surfaces are shown in Table 3.2. It shows that electron transfer from metal to H_2 which is adsorbed on MG surfaces. Charges of metals of MGs were found to be in order: Fe (Z=2.14) > Ni (Z=1.54) ~ Co (Z=1.53) > Au (Z=1.10) > Sc (Z=0.46) > Zn (Z=0.34) > Ti (Z=0.19). The electron transfer on metals correspond to the adsorption abilities of their MGs on hydrogen molecule.

The shortest bond-distances between atoms of H_2 and surface atoms of the transition metal doped and non-doped graphenes are shown in Table 3.3. It shows that shortest bond-distances of adsorption configurations are in order: C···H2 > Sc···H1 (Sc···H2) > Zn···H1 > Ti···H1 (Ti···H2) > Au···H1 (Au···H2) > Co···H2 > Fe···H1 > Ni···H2. Alignments of adsorbing hydrogen molecule adsorbed on the Sc-G, Ti-G and Au-G surfaces were found to be parallel to the surface. Nevertheless, alignments of adsorbing hydrogen molecule adsorbed on the Ni-G and Zn-G surfaces were found to be approximately parallel to the surface.

Table 3.2 Mülliken charges of related atoms of clean and H_2 molecule adsorbed surfaces.

Compound	Adsorbent partial charge [a]						
	Clean			H_2 adsorbed surfaces			
	C1	**C2**	**C3**	**Metal**	**C1**	**C2**	**C3**
pristine	0.00	0.00	0.00	0.00	0.00	0.00	0.00
Sc-doped G	-0.23	-0.25	-0.25	0.46	-0.22	-0.24	-0.24
Ti-doped G	-0.20	-0.19	-0.19	0.19	-0.21	-0.21	-0.21
Fe-doped G	-0.28	-0.28	-0.28	2.14	-0.39	-0.38	-0.34
Co-doped G	-0.25	-0.24	-0.24	1.53	-0.32	-0.35	-0.32
Ni-doped G	-0.27	-0.26	-0.26	1.54	-0.26	-0.35	-0.31
Zn-doped G	-0.18	-0.24	-0.19	0.34	-0.18	-0.24	-0.19
Au-doped G	-0.15	-0.19	-0.13	1.10	-0.11	-0.27	-0.27

[a] In e.

Table 3.3 The shortest bond-distances between specific atoms of H_2 and surface atoms of the transition metal doped and non-doped graphenes.

Configuration/bonds	Bond distances (Å)
H_2/G	
C···H1	3.43
C···H2	3.18
H_2/Sc-G	
Sc···H1	2.45
Sc···H2	2.45
H_2/Ti-G	
Ti···H1	2.40
Ti···H2	2.40
H_2/Fe-G	
Fe···H1	1.53
Fe···H2	1.58
H_2/Co-G	
Co···H1	1.59
Co···H2	1.56
H_2/Ni-G	
Ni···H1	1.52
Ni···H2	1.51
H_2/Zn-G	
Zn···H1	2.44
Zn···H2	2.45
H_2/Au-G	
Au···H1	1.67
Au···H2	1.67

Plot of adsorption energy (ΔE_{ads}, eV) of hydrogen molecule on pristine and metal-doped graphenes are shown in Figure 3.3. It shows that hydrogen molecule adsorbed on the Fe-doped graphene is obviously the highest strength of which adsorption energy is -66.85 kcal/mol.

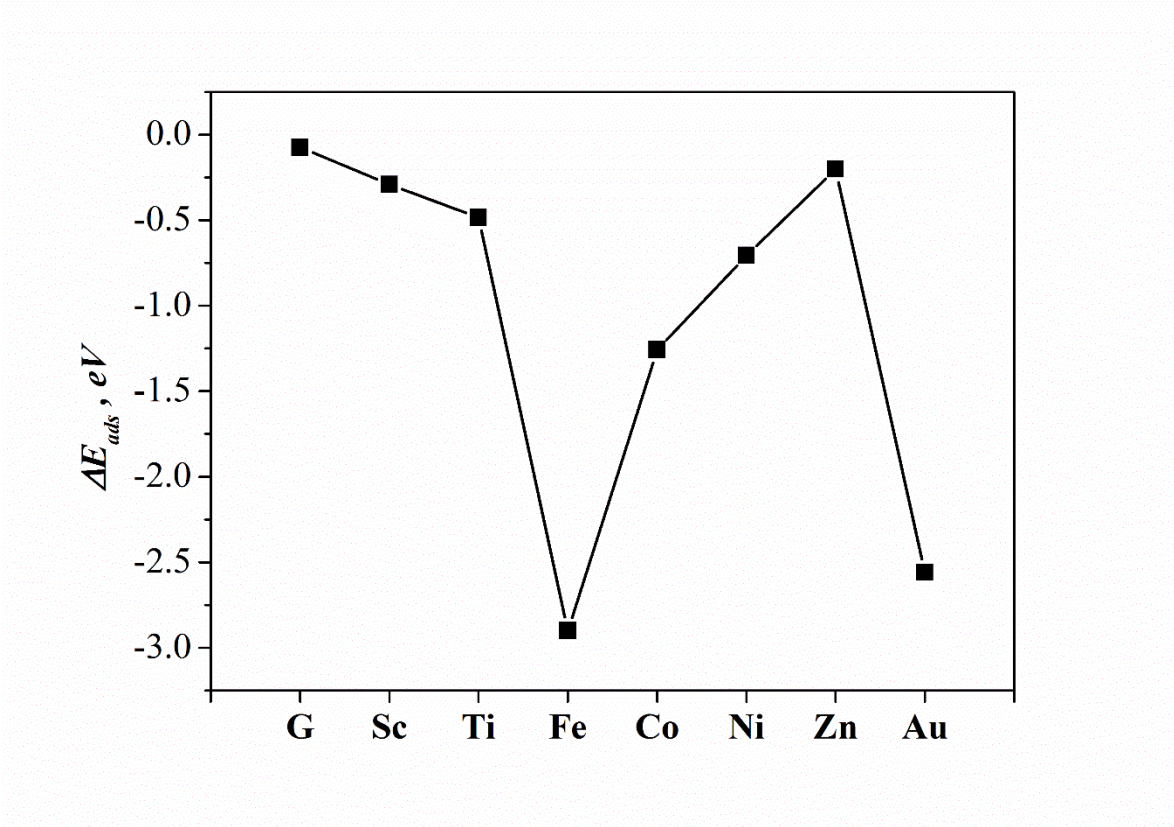

Figure 3.3 Plot of adsorption energy ($\Delta E_{ads}, eV$) of hydrogen molecule on pristine and metal-doped graphenes.

3.3 The optimized structures of metal doped and non-doped graphenes with H_2O

The SCC-DFTB-optimized structures of H_2O adsorbed on the transition metal doped graphene derivatives, Sc-, Ti-, Fe-, Co-, Ni-, Zn- and Au-doped G are shown in Figure 3.4. It shows that H_2O adsorbed all configurations are physical adsorption. Adsorption abilities on H_2O of metal doped graphene derivatives are in order: TiG > FeG > CoG > ScG > ZnG > NiG > AuG > G.

Adsorption energies of the SCC-DFTB-optimized structure of H_2O adsorbed on the transition metal doped graphene derivatives compared with graphene and energy gaps of their adsorption structures and energy–gap changes (in %) compared with clean MG, are shown in Table 3.4. As FeG is able to strongly adsorb water molecule with high energy–gap change (ΔE_g =66.67%), the FeG can therefore be performed as water sensor.

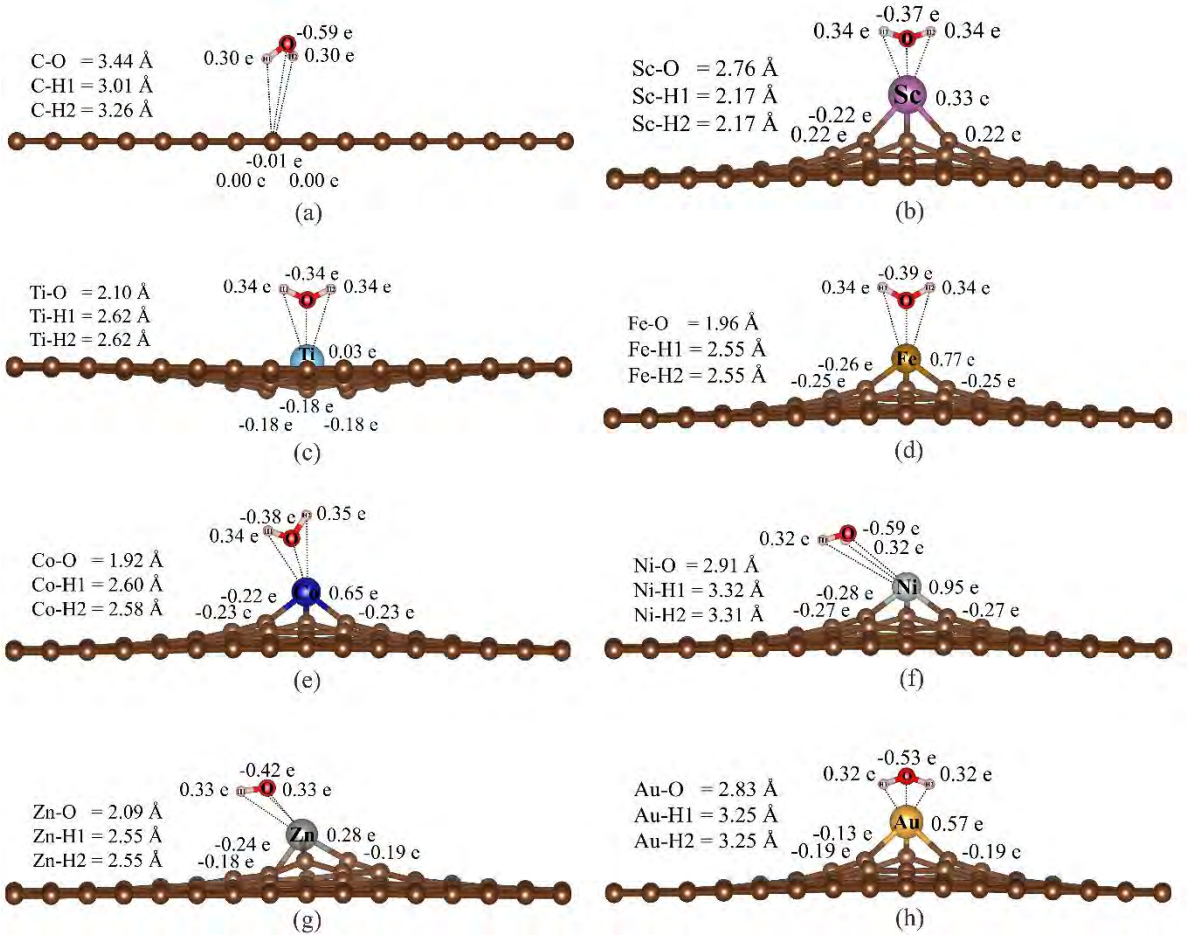

Figure 3.4 Adsorption of H_2O molecule on (a) pristine, (b) Sc-doped G, (c) Ti-doped G, (d) Fe-doped G, (e) Co-doped G, (f) Ni-doped G, (g) Zn-doped G and (h) Au-doped G. Mülliken charges of related atoms and bond distances between H_2O molecule and doped atom are shown.

Table 3.4 Adsorption energies of H_2O adsorbed on the transition metal doped graphene derivatives compared with graphene and energy gaps of their adsorption structures, computed by the SCC-DFTB method.

Adsorption	ΔE_{ads}[a]	E_g[b]	ΔE_g[c]
G	-	1.71	-
H_2O + G → H_2O/G	-3.14	1.70	-0.58
Sc-G	-	0.87	-
H_2O + Sc-G → H_2O/Sc-G	-32.11	0.83	-4.60
Ti-G	-	0.89	-
H_2O + Ti-G → H_2O/Ti-G	-62.17	0.86	-3.37
Fe-G	-	0.21	-
H_2O + Fe-G → H_2O/Fe-G	-51.15	0.35	66.67
Co-G	-	0.54	-
H_2O + Co-G → H_2O/Co-G	-34.85	0.14	-74.07
Ni-G	-	0.62	-
H_2O + Ni-G → H_2O/Ni-G	-11.63	0.11	-82.26
Zn-G	-	0.66	-
H_2O + Zn-G → H_2O/Zn-G	-29.70	0.70	6.06
Au-G	-	0.35	-
H_2O + Au-G → H_2O/Au-G	-9.25	0.26	-25.71

[a] At 298.15 K, in kcal/mol.

[b] In eV.

[c] Percentage of energy–gap change compared with clean MG.

Mülliken charges of related atoms of clean and H_2O molecule adsorbed surfaces are shown in Table 3.5. It shows that electron transfer from metal to H_2O which is adsorbed on MG surfaces. Charges of metals of MGs were found to be in order: Ni (Z=0.95) > Fe (Z=0.77) > Co (Z=0.65) > Au (Z=0.57) > Sc (Z=0.33) > Zn (Z=0.28) > Ti (Z=0.03). The electron transfer on metals correspond to the adsorption abilities of their MGs on water molecule.

The shortest bond-distances between atoms of H_2O and surface atoms of the transition metal doped and non-doped graphenes are shown in Table 3.6. It shows that shortest bond-distances of adsorption configurations are in order: C···H2 > Ni···O > Au···O > Sc···O > Ti···O ~ Zn···O > Fe···O > Co···O. Alignments of adsorbing water molecule adsorbed on the Sc-G, Ti-G, Fe-G, Zn-G and Au-G surfaces were found to be parallel to the surface. Nevertheless, alignments of adsorbing water molecule adsorbed on the Ni-G surfaces were found to be approximately parallel to the surface.

Table 3.5 Mülliken charges of related atoms of clean and H_2O molecule adsorbed surfaces

Compound	adsorbent partial charge [a]						
	Clean			H_2O adsorbed surfaces			
	C1	**C2**	**C3**	**Metal**	**C1**	**C2**	**C3**
pristine	0.00	0.00	0.00	0.00	-0.01	-0.01	-0.01
Sc-doped G	-0.23	-0.25	-0.25	0.33	-0.22	-0.22	-0.22
Ti-doped G	-0.20	-0.19	-0.19	0.03	-0.18	-0.18	-0.18
Fe-doped G	-0.28	-0.28	-0.28	0.77	-0.26	-0.25	-0.25
Co-doped G	-0.25	-0.24	-0.24	0.65	-0.22	-0.23	-0.23
Ni-doped G	-0.27	-0.26	-0.26	0.95	-0.28	-0.27	-0.27
Zn-doped G	-0.18	-0.24	-0.19	0.28	-0.24	-0.18	-0.19
Au-doped G	-0.15	-0.19	-0.13	0.57	-0.13	-0.19	-0.19

[a] In e.

Table 3.6 The shortest bond-distances between specific atoms of H_2O and surface atoms of the transition metal doped and non-doped graphenes

Configuration/bonds	Bond distances (Å)
H_2O/G	
C···H1	3.26
C···H2	3.01
C···O	3.44
H_2O/Sc-G	
Sc···H1	2.76
Sc···H2	2.76
Sc···O	2.17
H_2O/Ti-G	
Ti···H1	2.62
Ti···H2	2.62
Ti···O	2.10
H_2O/Fe-G	
Fe···H1	2.55
Fe···H2	2.55
Fe···O	1.96
H_2/Co-G	
Co···H1	2.60
Co···H2	2.58
Co···O	1.92
H_2O/Ni-G	
Ni···H1	3.32
Ni···H2	3.31
Ni···O	2.91
H_2O/Zn-G	
Zn···H1	2.55
Zn···H2	2.55
Zn···O	2.09
H_2O/Au-G	
Au···H1	3.25
Au···H2	3.25
Au···O	2.83

Plot of adsorption energy (ΔE_{ads}, eV) of water molecule on pristine and metal-doped graphenes are shown in Figure 3.5. It shows that water molecule adsorbed on the Ti-doped graphene is obviously the highest strength of which adsorption energy is -62.17 kcal/mol.

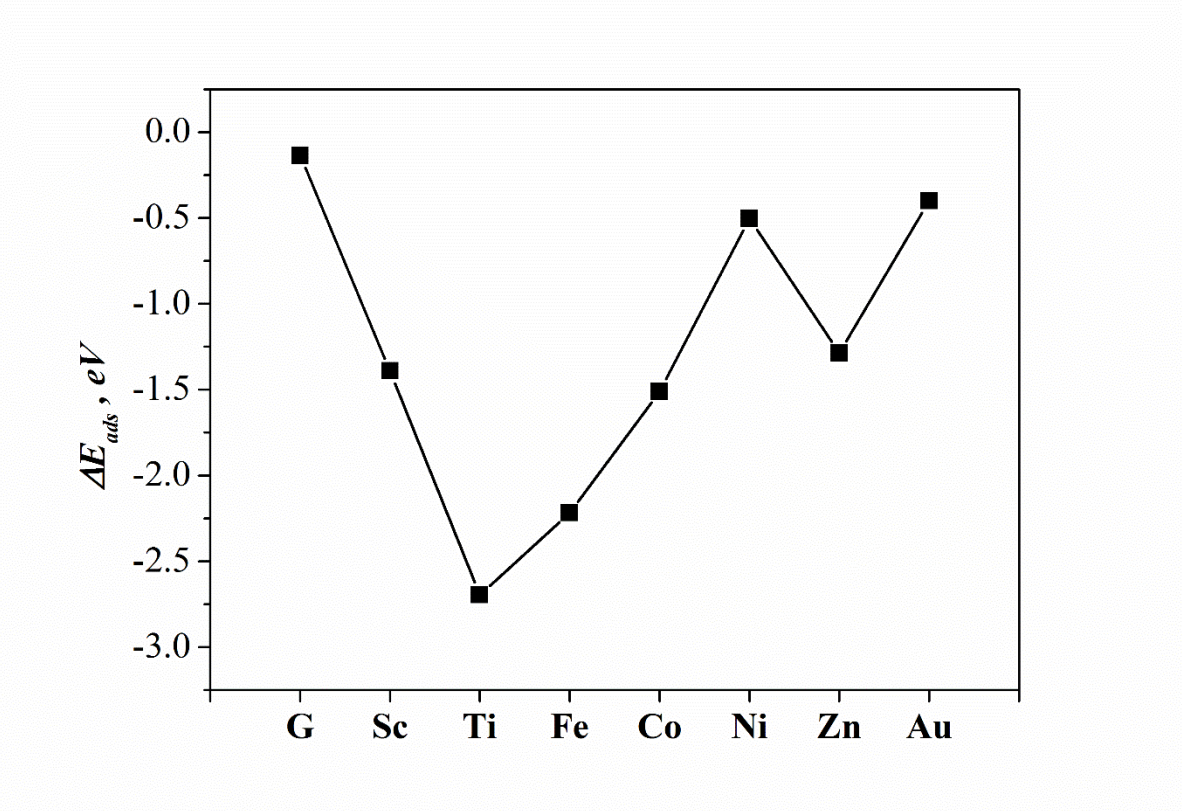

Figure 3.5 Plot of adsorption energy ($\Delta E_{ads}, eV$) of water molecule on pristine and metal-doped graphenes.

3.4 The optimized structures of metal doped and non-doped graphenes with N_2O pointing with N-end

The SCC-DFTB-optimized structures of N_2O pointing with N-end adsorbed on the transition metal doped graphene derivatives, Sc-, Ti-, Fe-, Co-, Ni-, Zn- and Au-doped G are shown in Figure 3.6. It shows that N_2O pointing with N-end adsorbed all configurations are physical adsorption. NiG is only configuration of not adsorption. Adsorption abilities on N_2O pointing with N-end of metal doped graphene derivatives are in order: CoG > ZnG > FeG > ScG > TiG > AuG > G.

Adsorption energies of the SCC-DFTB-optimized structure of N_2O pointing with N-end adsorbed on the transition metal doped graphene derivatives compared with graphene and energy gaps of their adsorption structures and energy–gap changes (in %) compared with clean MG, are shown in Table 3.7. As FeG is able to strongly adsorb nitrogen dioxide molecule pointing with N-end with high energy–gap change (ΔE_g =285.71%), the FeG can therefore be performed as nitrogen dioxide gas sensor.

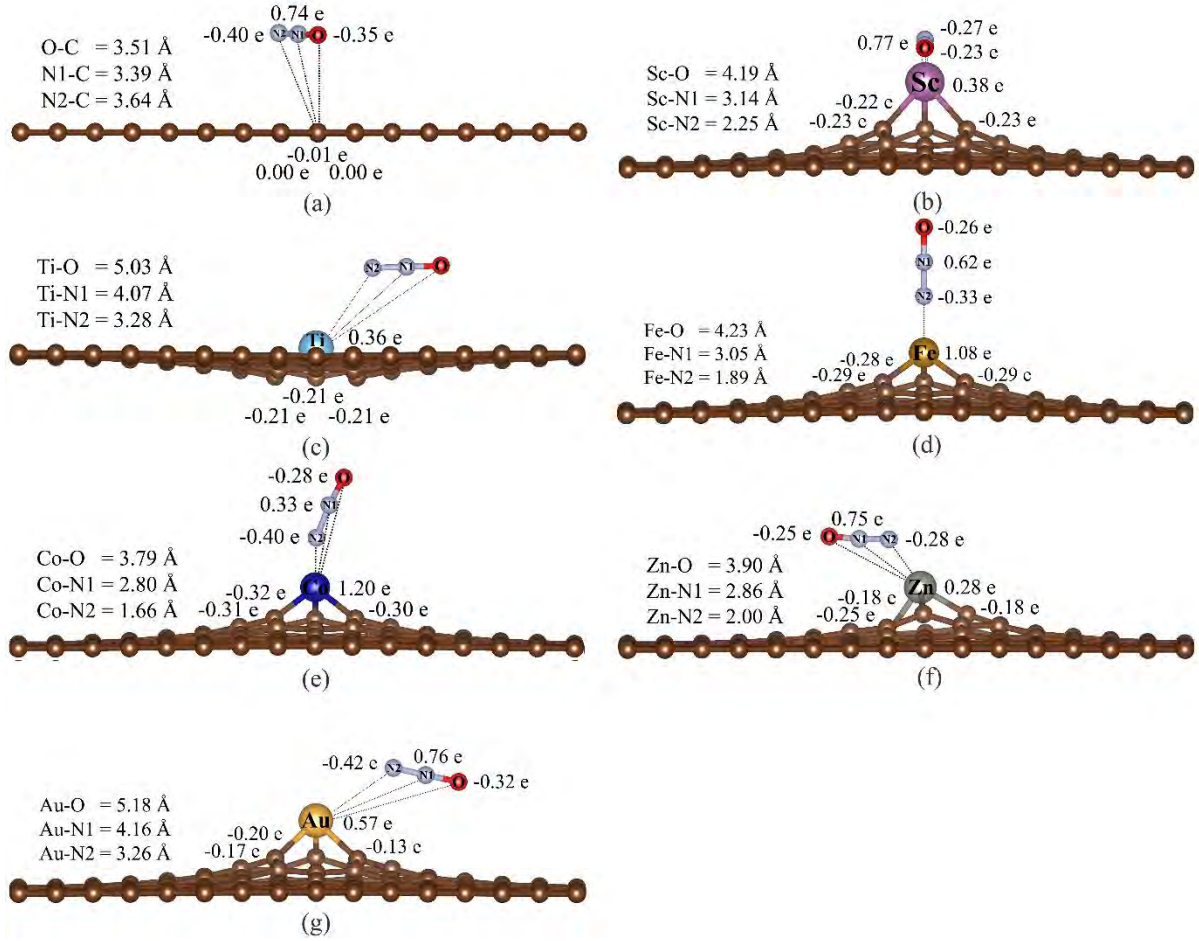

Figure 3.6 Adsorption of N_2O molecule as [M· · ·N=N=O], configuration I on (a) pristine, (b) Sc-doped G, (c) Ti-doped G, (d) Fe-doped G, (e) Co-doped G, (f) Zn-doped G and (g) Au-doped G. Mülliken charges of related atoms and bond distances between N_2O pointing with N-end molecule and doped atom are shown.

Table 3.7 Adsorption energies of N_2O molecule pointing with N-end adsorbed on the transition metal doped graphene derivatives compared with graphene and energy gaps of their adsorption structures, computed by the SCC-DFTB method.

Adsorption	ΔE_{ads}[a]	E_g[b]	ΔE_g[c]
G	-	1.71	-
$\underline{N}_2O$ + G → $\underline{N}_2O$/G	-4.00	1.71	0.00
Sc-G	-	0.87	-
$\underline{N}_2O$ + Sc-G → $\underline{N}_2O$/Sc-G	-19.06	1.02	17.24
Ti-G	-	0.89	-
$\underline{N}_2O$ + Ti-G → $\underline{N}_2O$/Ti-G	-15.07	1.14	28.09
Fe-G	-	0.21	-
$\underline{N}_2O$ + Fe-G → $\underline{N}_2O$/Fe-G	-20.29	0.81	285.71
Co-G	-	0.54	-
$\underline{N}_2O$ + Co-G → $\underline{N}_2O$/Co-G	-54.64	0.92	70.37
Ni-G	-	0.62	-
$\underline{N}_2O$ + Ni-G → $\underline{N}_2O$/Ni-G	-	-	-
Zn-G	-	0.66	-
$\underline{N}_2O$ + Zn-G → $\underline{N}_2O$/Zn-G	-36.72	0.76	15.15
Au-G	-	0.35	-
$\underline{N}_2O$ + Au-G → $\underline{N}_2O$/Au-G	-14.16	0.13	-62.86

[a] At 298.15 K, in kcal/mol.

[b] In eV.

[c] Percentage of energy–gap change compared with clean MG.

Mülliken charges of related atoms of clean and N_2O molecule pointing with N-end adsorbed surfaces are shown in Table 3.8. It shows that electron transfer from metal to N_2O molecule pointing with N-end which is adsorbed on MG surfaces. Charges of metals of MGs were found to be in order: Co (Z=1.20) > Fe (Z=1.08) > Au (Z=0.57) > Sc (Z=0.38) > Ti (Z=0.36) > Zn (Z=0.28). The electron transfer on metals correspond to the adsorption abilities of their MGs on N_2O molecule pointing with N-end.

The shortest bond-distances between atoms of N_2O molecule pointing with N-end and surface atoms of the transition metal doped and non-doped graphenes are shown in Table 3.9. It shows that shortest bond-distances of adsorption configurations are in order: C···N1 > Ti···N2 > Au···N2 > Sc···N2 > Zn···N2 > Fe···N2 > Co···N2. Alignments of adsorbing N_2O molecule adsorbed on the G, Sc-G, Ti-G, Zn-G and Au-G surfaces were found to be approximately parallel to the surface. An adsorbing N_2O molecule aligns by pointing its N-end toward the metal of the Fe-G and Co-G surfaces and approximately perpendicular to the surface.

Table 3.8 Mülliken charges of related atoms of clean and N_2O molecule pointing with N-end adsorbed surfaces

Compound	adsorbent partial charge [a]						
	Clean			N_2O adsorbed surfaces			
	C1	**C2**	**C3**	**Metal**	**C1**	**C2**	**C3**
pristine	0.00	0.00	0.00	0.00	-0.01	-0.01	0.00
Sc-doped G	-0.23	-0.25	-0.25	0.38	-0.22	-0.23	-0.23
Ti-doped G	-0.20	-0.19	-0.19	0.36	-0.21	-0.21	-0.21
Fe-doped G	-0.28	-0.28	-0.28	1.08	-0.28	-0.29	-0.29
Co-doped G	-0.25	-0.24	-0.24	1.20	-0.30	-0.32	-0.31
Ni-doped G	-	-	-	-	-	-	-
Zn-doped G	-0.18	-0.24	-0.19	0.28	-0.18	-0.25	-0.18
Au-doped G	-0.15	-0.19	-0.13	0.57	-0.20	-0.13	-0.17

[a] In e.

Table 3.9 The shortest bond-distances between specific atoms of N_2O molecule pointing with N-end and surface atoms of the transition metal doped and non-doped graphenes

Configuration/bonds	Bond distances (Å)
$\underline{N_2}O$/G	
C···N1	3.39
C···N2	3.64
C···O	3.51
$\underline{N_2}O$/Sc-G	
Sc···N1	3.14
Sc···N2	2.25
Sc···O	4.19
$\underline{N_2}O$/Ti-G	
Ti···N1	4.07
Ti···N2	3.28
Ti···O	5.03
$\underline{N_2}O$/Fe-G	
Fe···N1	3.05
Fe···N2	1.89
Fe···O	4.23
N_2O/Co-G	
Co···N1	2.80
Co···N2	1.66
Co···O	3.79
$\underline{N_2}O$/Ni-G	
Ni···N1	-
Ni···N2	-
Ni···O	-
$\underline{N_2}O$/Zn-G	
Zn···N1	2.86
Zn···N2	2.00
Zn···O	3.90
$\underline{N_2}O$/Au-G	
Au···N1	4.16
Au···N2	3.26
Au···O	5.18

Plot of adsorption energy (ΔE_{ads}, eV) of N_2O molecule pointing with N-end on pristine and metal-doped graphenes are shown in Figure 3.7. It shows that nitrogen dioxide molecule adsorbed on the Co-doped graphene is obviously the highest strength of which adsorption energy is -54.64 kcal/mol.

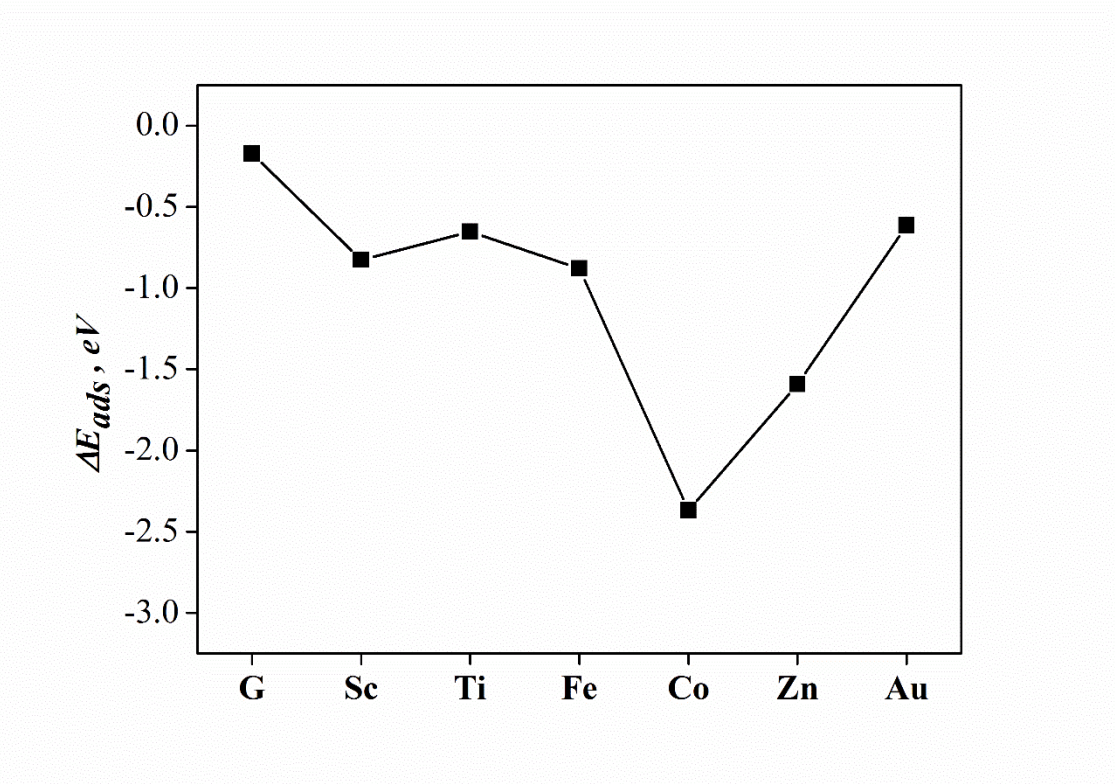

Figure 3.*7* Plot of adsorption energy ($\Delta E_{ads}, eV$) of N_2O molecule as [M· · ·N=N=O] on pristine and metal-doped graphenes.

3.5 The optimized structures of metal doped and non-doped graphenes with N_2O pointing with O-end

The SCC-DFTB-optimized structures of N_2O pointing with O-end adsorbed on the transition metal doped graphene derivatives, Sc-, Ti-, Fe-, Co-, Ni-, Zn- and Au-doped G are shown in Figure 3.8. It shows that N_2O pointing with O-end adsorbed on G, ScG, TiG, FeG, ZnG and AuG are physical adsorption and CoG is dissociative chemisorption. NiG is only configuration of not adsorption. Adsorption abilities on N_2O pointing with O-end of metal doped graphene derivatives are in order: CoG > TiG > FeG > ZnG > ScG > AuG > G.

Adsorption energies of the SCC-DFTB-optimized structure of N_2O pointing with O-end adsorbed on the transition metal doped graphene derivatives compared with graphene and energy gaps of their adsorption structures and energy–gap changes (in %) compared with clean MG, are shown in Table 3.10. As FeG is able to strongly adsorb nitrogen dioxide molecule pointing with O-end with high energy–gap change (ΔE_g =238.10%), the FeG can therefore be performed as nitrogen dioxide gas sensor.

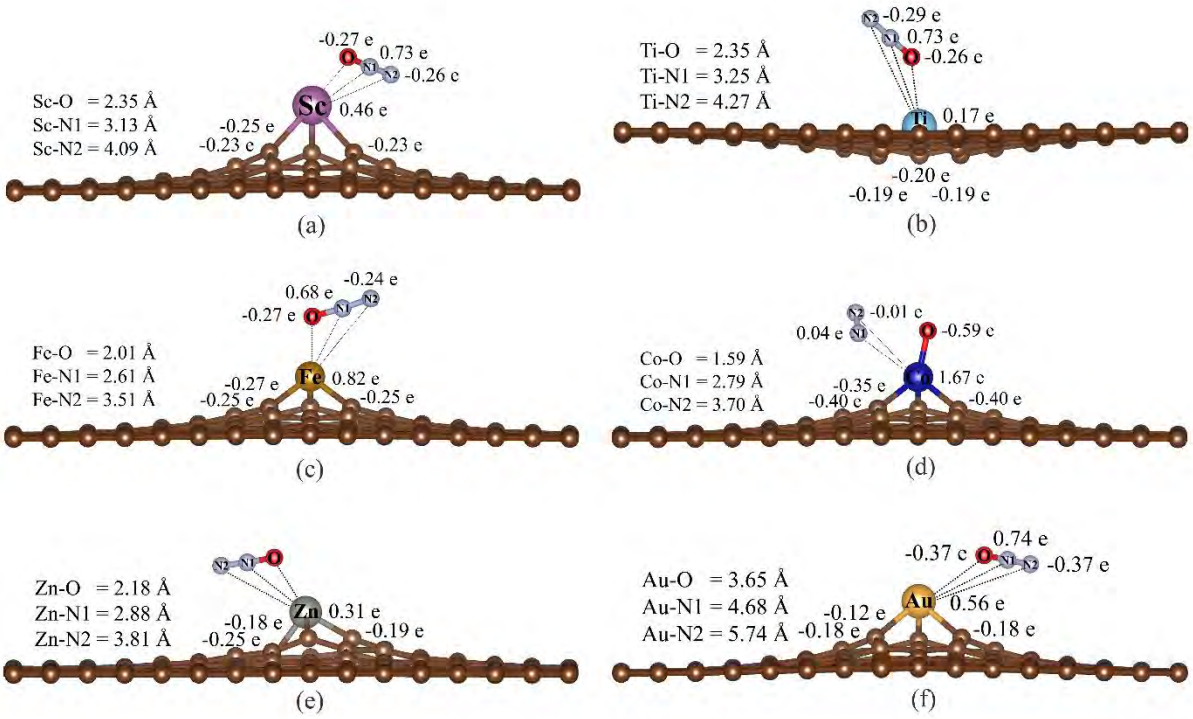

Figure 3.8 Adsorption of N_2O molecule as [M· · ·O=N=N], configuration II on (a) Sc-doped G, (b) Ti-doped G, (c) Fe-doped G, (d) Co-doped G, (e) Zn-doped G and (f) Au-doped G. Mülliken charges of related atoms and bond distances between N_2O pointing with O-end molecule and doped atom are shown.

Table 3.10 Adsorption energies of N_2O molecule pointing with O-end adsorbed on the transition metal doped graphene derivatives compared with graphene and energy gaps of their adsorption structures, computed by the SCC-DFTB method.

Adsorption	ΔE_{ads}[a]	E_g[b]	ΔE_g[c]
G	-	1.71	-
N_2O + G → N_2O/G	-4.00	1.71	0.00
Sc-G	-	0.87	-
N_2O + Sc-G → N_2O/Sc-G	-23.79	1.11	27.59
Ti-G	-	0.89	-
N_2O + Ti-G → N_2O/Ti-G	-50.82	1.13	26.97
Fe-G	-	0.21	-
N_2O + Fe-G → N_2O/Fe-G	-43.60	0.71	238.10
Co-G	-	0.54	-
N_2O + Co-G → N_2O/Co-G	-126.67	1.15	112.96
Ni-G	-	0.62	-
N_2O + Ni-G → N_2O/Ni-G	-	-	-
Zn-G	-	0.66	-
N_2O + Zn-G → N_2O/Zn-G	-26.06	0.76	15.15
Au-G	-	0.35	-
N_2O + Au-G → N_2O/Au-G	-13.16	0.16	-54.29

[a] At 298.15 K, in kcal/mol.

[b] In eV.

[c] Percentage of energy–gap change compared with clean MG.

Mülliken charges of related atoms of clean and N_2O molecule pointing with O-end adsorbed surfaces are shown in Table 3.11. It shows that electron transfer from metal to N_2O molecule pointing with O-end which is adsorbed on MG surfaces. Charges of metals of MGs were found to be in order: Co (Z=1.67) > Fe (Z=0.82) > Au (Z=0.56) > Sc (Z=0.46) > Zn (Z=0.31) > Ti (Z=0.17). The electron transfer on metals correspond to the adsorption abilities of their MGs on N_2O molecule pointing with O-end.

The shortest bond-distances between atoms of N_2O molecule pointing with O-end and surface atoms of the transition metal doped and non-doped graphenes are shown in Table 3.12. It shows that shortest bond-distances of adsorption configurations are in order: Au···O > C···N1 > Sc···O = Ti···O > Zn···O > Fe···O > Co···O. It was found that an adsorbing N_2O molecule aligns by pointing its O-end toward a metal of all the surfaces, except Co-G which N_2O is dissociative adsorbed on Co atom.

Table 3.11 Mülliken charges of related atoms of clean and N_2O molecule pointing with O-end adsorbed surfaces

Compound	adsorbent partial charge [a]						
	Clean			N2O adsorbed surfaces			
	C1	**C2**	**C3**	**Metal**	**C1**	**C2**	**C3**
pristine	0.00	0.00	0.00	0.00	-0.01	-0.01	0.00
Sc-doped G	-0.23	-0.25	-0.25	0.46	-0.25	-0.23	-0.23
Ti-doped G	-0.20	-0.19	-0.19	0.17	-0.20	-0.19	-0.19
Fe-doped G	-0.28	-0.28	-0.28	0.82	-0.25	-0.25	-0.27
Co-doped G	-0.25	-0.24	-0.24	1.67	-0.40	-0.40	-0.35
Ni-doped G	-	-	-	-	-	-	-
Zn-doped G	-0.18	-0.24	-0.19	0.31	-0.19	-0.25	-0.18
Au-doped G	-0.15	-0.19	-0.13	0.56	-0.12	-0.18	-0.18

[a] In e.

Table 3.12 The shortest bond-distances between specific atoms of N_2O molecule pointing with O-end and surface atoms of the transition metal doped and non-doped graphenes

Configuration/bonds	Bond distances (Å)
$N_2\underline{O}$/G	
C···N1	3.39
C···N2	3.64
C···O	3.51
$N_2\underline{O}$/Sc-G	
Sc···N1	3.13
Sc···N2	4.09
Sc···O	2.35
$N_2\underline{O}$/Ti-G	
Ti···N1	3.25
Ti···N2	4.27
Ti···O	2.35
$N_2\underline{O}$/Fe-G	
Fe···N1	2.61
Fe···N2	3.51
Fe···O	2.01
$N_2\underline{O}$/Co-G	
Co···N1	2.79
Co···N2	3.70
Co···O	1.59
$N_2\underline{O}$/Ni-G	
Ni···N1	-
Ni···N2	-
Ni···O	-
$N_2\underline{O}$/Zn-G	
Zn···N1	2.88
Zn···N2	3.81
Zn···O	2.18
$N_2\underline{O}$/Au-G	
Au···N1	4.68
Au···N2	5.74
Au···O	3.65

Plot of adsorption energy (ΔE_{ads}, eV) of N_2O molecule pointing with O-end on pristine and metal-doped graphenes are shown in Figure 3.9. It shows that nitrogen dioxide molecule adsorbed on the Co-doped graphene is obviously the highest strength of which adsorption energy is -126.67 kcal/mol.

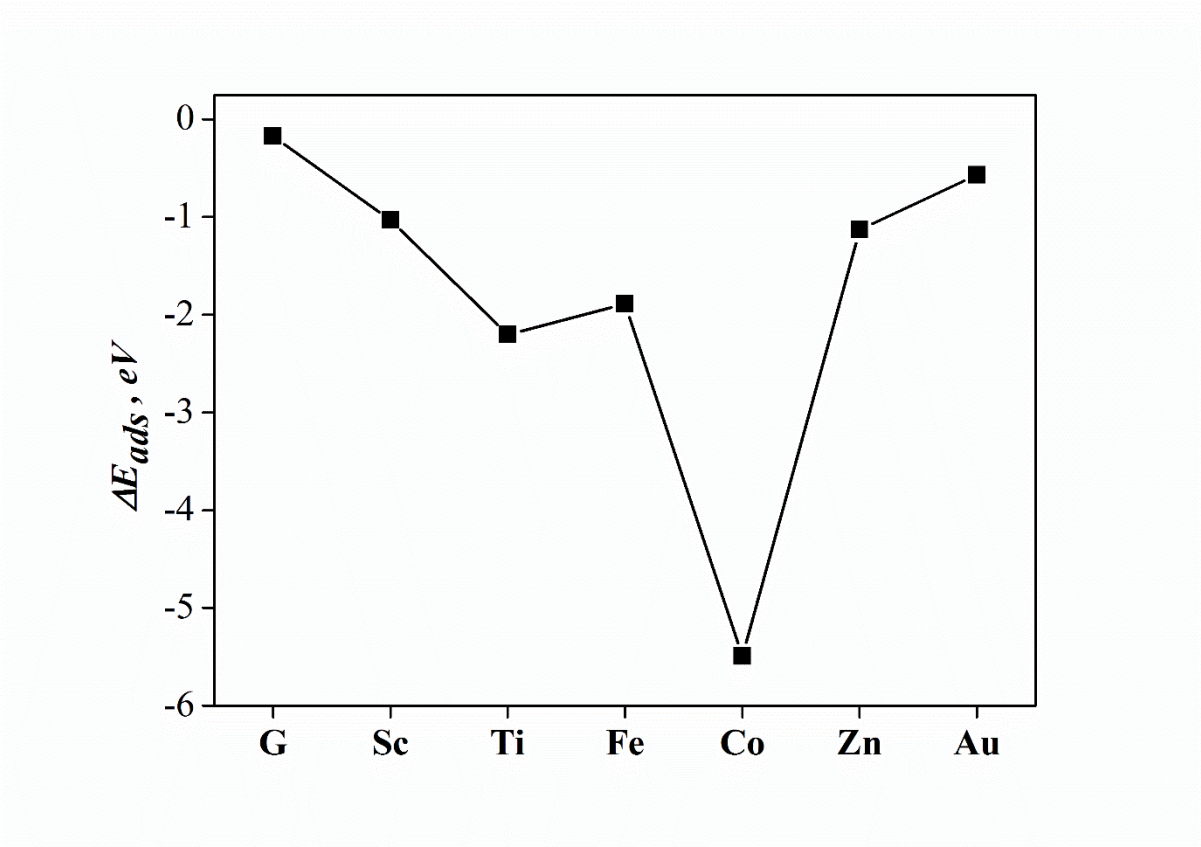

Figure 3.9 Plot of adsorption energy ($\Delta E_{ads}, eV$) of N_2O molecule as [M· · ·O=N=N], on pristine and metal-doped graphenes.

3.6 The optimized structures of metal doped and non-doped graphenes with CO pointing with C-end

The SCC-DFTB-optimized structures of CO pointing with C-end adsorbed on the transition metal doped graphene derivatives, Sc-, Ti-, Fe-, Co-, Ni-, Zn- and Au-doped G are shown in Figure 3.10. It shows that CO pointing with C-end adsorbed all configurations are physical adsorption. Adsorption abilities on CO pointing with C-end of metal doped graphene derivatives are in order: TiG > CoG > FeG > AuG > NiG > ZnG > ScG > G.

Adsorption energies of the SCC-DFTB-optimized structure of CO pointing with C-end adsorbed on the transition metal doped graphene derivatives compared with graphene and energy gaps of their adsorption structures and energy–gap changes (in %) compared with clean MG, are shown in Table 3.13. As FeG is able to strongly adsorb carbon monoxide molecule pointing with C-end with high energy–gap change (ΔE_g =333.33%), the FeG can therefore be performed as carbon monoxide gas sensor.

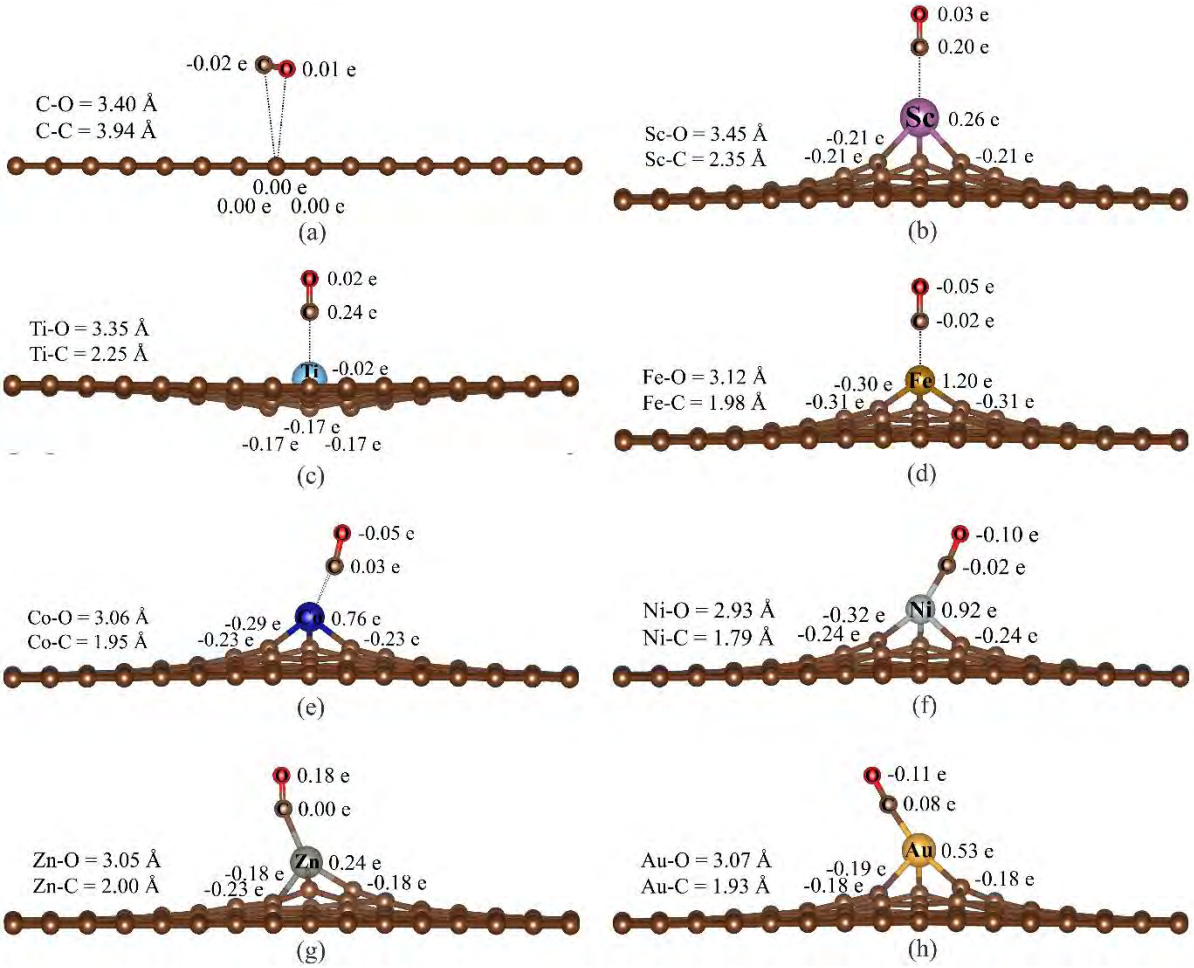

Figure 3.10 Adsorption of CO molecule as [M· · ·C=O], configuration I on (a) pristine, (b) Sc-doped G, (c) Ti-doped G, (d) Fe-doped G, (e) Co-doped G, (f) Ni-doped G, (g) Zn-doped G and (h) Au-doped G. Mülliken charges of related atoms and bond distances between CO pointing with C-end molecule and doped atom are shown.

Table 3.13 Adsorption energies of CO molecule pointing with C-end adsorbed on the transition metal doped graphene derivatives compared with graphene and energy gaps of their adsorption structures, computed by the SCC-DFTB method.

Adsorption	ΔE_{ads}[a]	E_g[b]	ΔE_g[c]
G	-	1.71	-
CO + G → CO/G	-3.01	1.71	0.00
Sc-G	-	0.87	-
CO + Sc-G → CO/Sc-G	-14.99	1.07	22.99
Ti-G	-	0.89	-
CO + Ti-G → CO/Ti-G	-48.21	1.08	21.35
Fe-G	-	0.21	-
CO + Fe-G → CO/Fe-G	-33.67	0.91	333.33
Co-G	-	0.54	-
CO + Co-G → CO/Co-G	-35.30	0.58	7.41
Ni-G	-	0.62	-
CO + Ni-G → CO/Ni-G	-27.52	0.41	-33.87
Zn-G	-	0.66	-
CO + Zn-G → CO/Zn-G	-27.32	0.78	18.18
Au-G	-	0.35	-
CO + Au-G → CO/Au-G	-33.18	0.38	8.57

[a] At 298.15 K, in kcal/mol.

[b] In eV.

[c] Percentage of energy–gap change compared with clean MG.

Mülliken charges of related atoms of clean and CO molecule pointing with C-end adsorbed surfaces are shown in Table 3.14. It shows that electron transfer from metal to CO molecule pointing with C-end which is adsorbed on MG surfaces. Charges of metals of MGs were found to be in order: Fe (Z=1.20) > Ni (Z=0.92) > Co (Z=0.76) > Au (Z=0.53) > Sc (Z=0.26) > Zn (Z=0.24) > Ti (Z=-0.02). The electron transfer on metals correspond to the adsorption abilities of their MGs on CO molecule pointing with C-end.

The shortest bond-distances between atoms of CO molecule pointing with C-end and surface atoms of the transition metal doped and non-doped graphenes are shown in Table 3.15. It shows that shortest bond-distances of adsorption configurations are in order: C···O > Sc···C > Ti···C > Zn···C > Fe···C > Co···C > Au···C > Ni···C. Alignment of adsorbing CO molecule adsorbed on the G surface was found to be approximately parallel to the surface. An adsorbing CO molecule aligns by pointing its C-end toward the metal of all the surfaces.

Table 3.14 Mülliken charges of related atoms of clean and CO molecule pointing with C-end adsorbed surfaces

Compound	adsorbent partial charge [a]						
	Clean			CO adsorbed surfaces			
	C1	**C2**	**C3**	**Metal**	**C1**	**C2**	**C3**
pristine	0.00	0.00	0.00	0.00	0.00	0.00	0.00
Sc-doped G	-0.23	-0.25	-0.25	0.26	-0.21	-0.21	-0.21
Ti-doped G	-0.20	-0.19	-0.19	-0.02	-0.17	-0.17	-0.17
Fe-doped G	-0.28	-0.28	-0.28	1.20	-0.30	-0.31	-0.31
Co-doped G	-0.25	-0.24	-0.24	0.76	-0.23	-0.29	-0.23
Ni-doped G	-0.27	-0.26	-0.26	0.92	-0.24	-0.32	-0.24
Zn-doped G	-0.18	-0.24	-0.19	0.24	-0.18	-0.23	-0.18
Au-doped G	-0.15	-0.19	-0.13	0.53	-0.18	-0.18	-0.19

[a] In e.

Table 3.15 The shortest bond-distances between specific atoms of CO molecule pointing with C-end and surface atoms of the transition metal doped and non-doped graphenes

Configuration/bonds	Bond distances (Å)
CO/G	
C···C	3.94
C···O	3.40
CO/Sc-G	
Sc···C	2.35
Sc···O	3.45
CO/Ti-G	
Ti···C	2.25
Ti···O	3.35
CO/Fe-G	
Fe···C	1.98
Fe···O	3.12
CO/Co-G	
Co···C	1.95
Co···O	3.06
CO/Ni-G	
Ni···C	1.79
Ni···O	2.93
CO/Zn-G	
Zn···C	2.00
Zn···O	3.05
CO/Au-G	
Au···C	1.93
Au···O	3.07

Plot of adsorption energy (ΔE_{ads}, eV) of CO molecule pointing with C-end on pristine and metal-doped graphenes are shown in Figure 3.11. It shows that carbon monoxide molecule adsorbed on the Ti-doped graphene is obviously the highest strength of which adsorption energy is -48.21 kcal/mol.

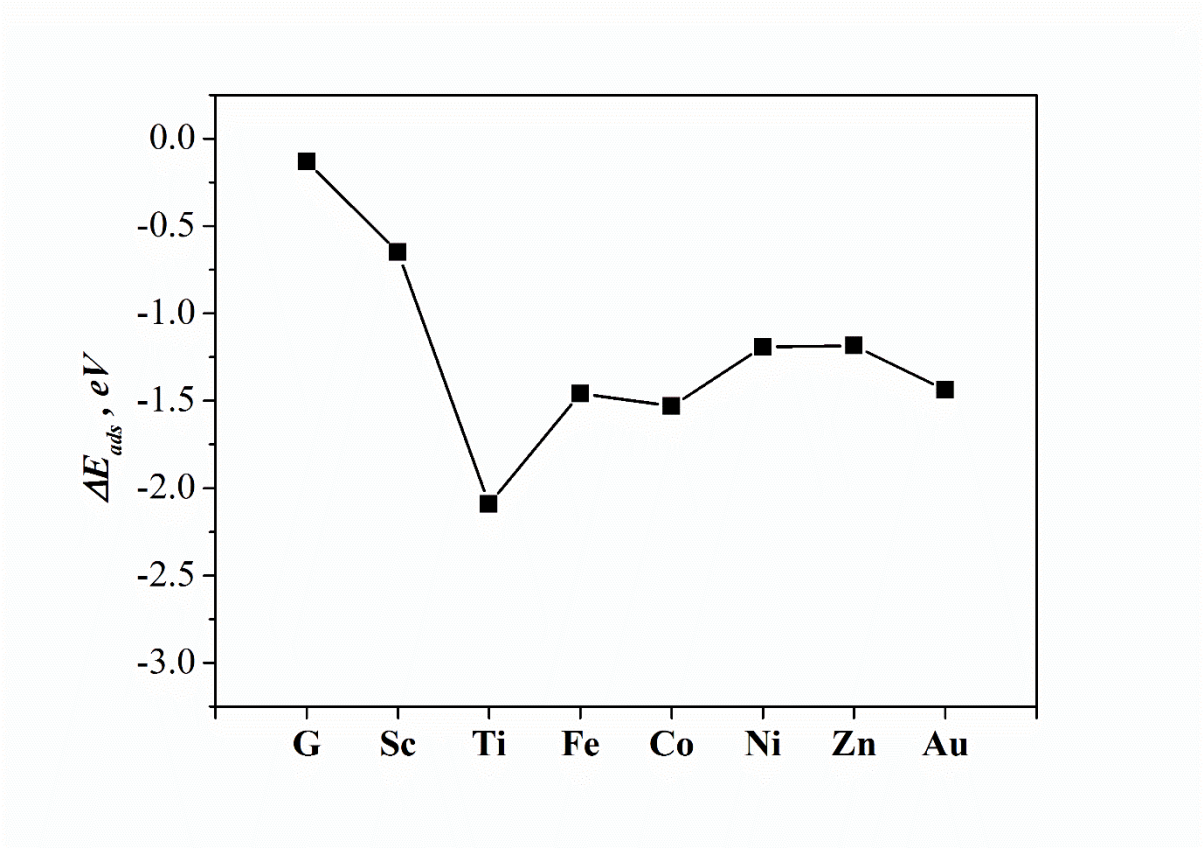

Figure 3.11 Plot of adsorption energy ($\Delta E_{ads}, eV$) of CO molecule as [M· · ·C=O] on pristine and metal-doped graphenes.

3.7 The optimized structures of metal doped and non-doped graphenes with CO pointing with O-end

The SCC-DFTB-optimized structures of CO pointing with O-end adsorbed on the transition metal doped graphene derivatives, Sc-, Ti-, Fe-, Co-, Ni-, Zn- and Au-doped G are shown in Figure 3.12. It shows that CO pointing with O-end adsorbed all configurations are physical adsorption. NiG is only configuration of not adsorption. Adsorption abilities on CO pointing with O-end of metal doped graphene derivatives are in order: TiG > FeG > CoG > ScG > ZnG > AuG > G.

Adsorption energies of the SCC-DFTB-optimized structure of CO pointing with O-end adsorbed on the transition metal doped graphene derivatives compared with graphene and energy gaps of their adsorption structures and energy–gap changes (in %) compared with clean MG, are shown in Table 3.16. As FeG is able to strongly adsorb carbon monoxide molecule pointing with O-end with high energy–gap change (ΔE_g =328.57%), the FeG can therefore be performed as carbon monoxide gas sensor.

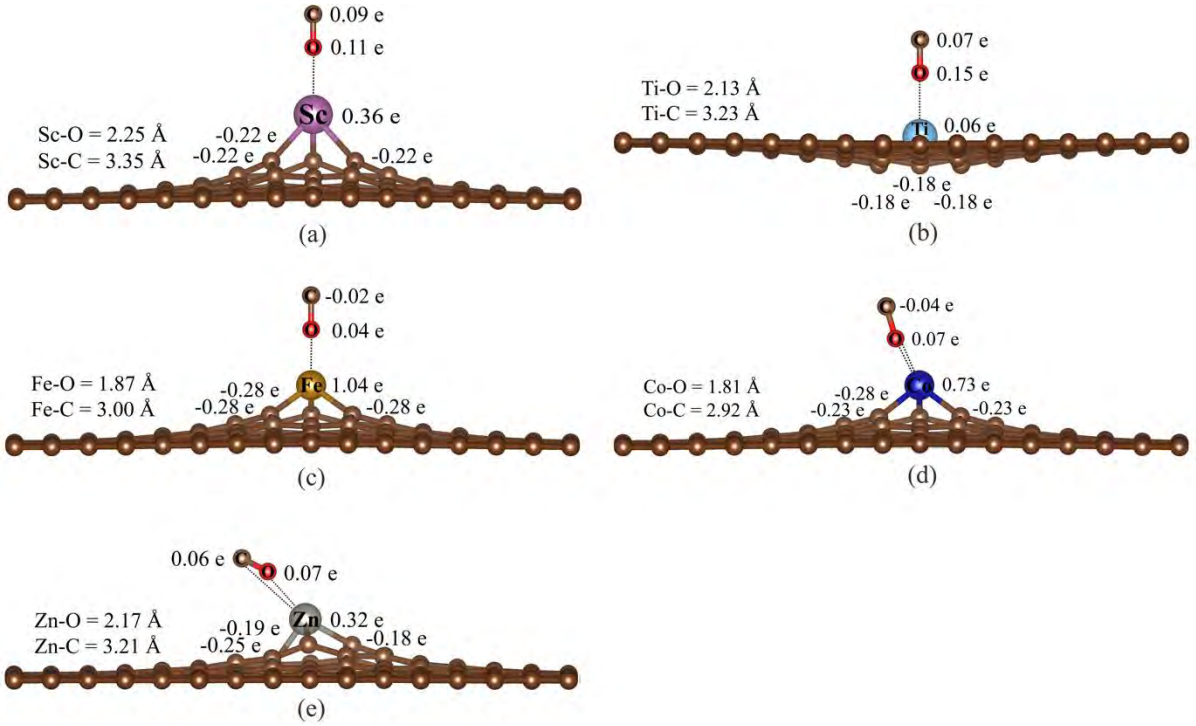

Figure 3.12 Adsorption of CO molecule as [M· · ·O=C], configuration II on (a) Sc-doped G, (b) Ti-doped G, (c) Fe-doped G, (d) Co-doped G and (e) Zn-doped G. Mülliken charges of related atoms and bond distances between CO pointing with O-end molecule and doped atom are shown.

Table 3.16 Adsorption energies of CO molecule pointing with O-end adsorbed on the transition metal doped graphene derivatives compared with graphene and energy gaps of their adsorption structures, computed by the SCC-DFTB method.

Adsorption	ΔE_{ads}[a]	E_g[b]	ΔE_g[c]
G	-	1.71	-
CO + G → CO/G	-3.01	1.71	0.00
Sc-G	-	0.87	-
CO + Sc-G → CO/Sc-G	-21.62	1.10	26.44
Ti-G	-	0.89	-
CO + Ti-G → CO/Ti-G	-52.09	1.10	23.60
Fe-G	-	0.21	-
CO + Fe-G → CO/Fe-G	-45.06	0.90	328.57
Co-G	-	0.54	-
CO + Co-G → CO/Co-G	-31.23	0.50	-7.41
Ni-G	-	0.62	-
CO + Ni-G → CO/Ni-G	-	-	-
Zn-G	-	0.66	-
CO + Zn-G → CO/Zn-G	-21.32	0.80	21.21
Au-G	-	0.35	-
CO + Au-G → CO/Au-G	-14.38	0.17	-51.43

[a] At 298.15 K, in kcal/mol.

[b] In eV.

[c] Percentage of energy–gap change compared with clean MG.

Mülliken charges of related atoms of clean and CO molecule pointing with O-end adsorbed surfaces are shown in Table 3.17. It shows that electron transfer from metal to CO molecule pointing with O-end which is adsorbed on MG surfaces. Charges of metals of MGs were found to be in order: Fe (Z=1.04) > Co (Z=0.73) > Au (Z=0.48) > Sc (Z=0.36) > Zn (Z=0.32) > Ti (Z=0.06). The electron transfer on metals correspond to the adsorption abilities of their MGs on CO molecule pointing with O-end.

The shortest bond-distances between atoms of CO molecule pointing with O-end and surface atoms of the transition metal doped and non-doped graphenes are shown in Table 3.18. It shows that shortest bond-distances of adsorption configurations are in order: C···O > Au···C > Sc···O > Zn···O > Ti···O > Fe···O > Co···O.

Table 3.17 Mülliken charges of related atoms of clean and CO molecule pointing with O-end adsorbed surfaces

Compound	adsorbent partial charge [a]						
	Clean			CO adsorbed surfaces			
	C1	**C2**	**C3**	**Metal**	**C1**	**C2**	**C3**
pristine	0.00	0.00	0.00	0.00	0.00	0.00	0.00
Sc-doped G	-0.23	-0.25	-0.25	0.36	-0.22	-0.22	-0.22
Ti-doped G	-0.20	-0.19	-0.19	0.06	-0.18	-0.18	-0.18
Fe-doped G	-0.28	-0.28	-0.28	1.04	-0.28	-0.28	-0.28
Co-doped G	-0.25	-0.24	-0.24	0.73	-0.23	-0.23	-0.28
Ni-doped G	-	-	-	-	-	-	-
Zn-doped G	-0.18	-0.24	-0.19	0.32	-0.19	-0.25	-0.18
Au-doped G	-0.15	-0.19	-0.13	0.48	-0.20	-0.19	-0.10

[a] In e.

Table 3.18 The shortest bond-distances between specific atoms of CO molecule pointing with O-end and surface atoms of the transition metal doped and non-doped graphenes

Configuration/bonds	Bond distances (Å)
CO/G	
C···C	3.94
C···O	3.40
CO/Sc-G	
Sc···C	3.35
Sc···O	2.25
CO/Ti-G	
Ti···C	3.23
Ti···O	2.13
CO/Fe-G	
Fe···C	3.00
Fe···O	1.87
CO/Co-G	
Co···C	2.92
Co···O	1.81
CO/Ni-G	
Ni···C	-
Ni···O	-
CO/Zn-G	
Zn···C	3.21
Zn···O	2.17
CO/Au-G	
Au···C	2.83
Au···O	3.93

Plot of adsorption energy (ΔE_{ads}, eV) of CO molecule pointing with O-end on pristine and metal-doped graphenes are shown in Figure 3.13. It shows that carbon monoxide molecule adsorbed on the Ti-doped graphene is obviously the highest strength of which adsorption energy is -52.09 kcal/mol.

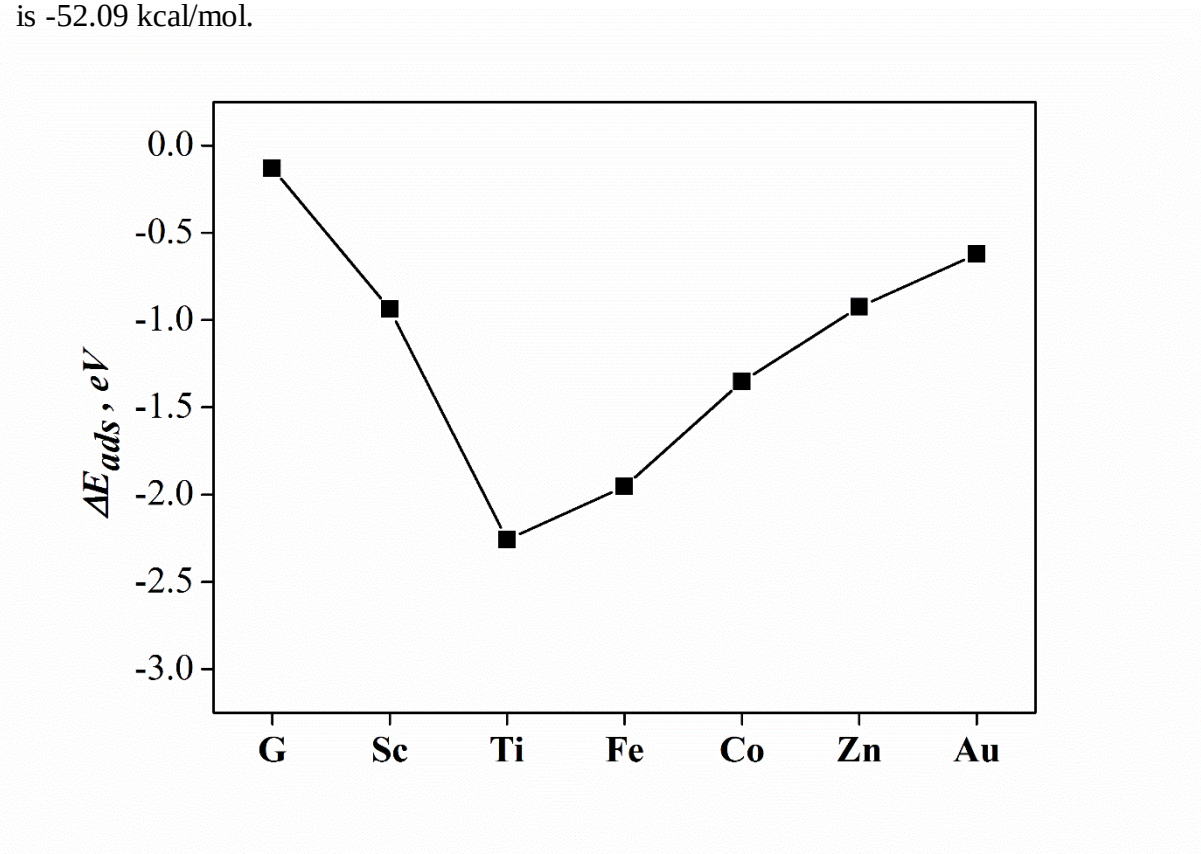

Figure 3.13 Plot of adsorption energy ($\Delta E_{ads}, eV$) of CO molecule as [M· · ·O=C] on pristine and metal-doped graphenes.

CHAPTER IV

CONCLUSION

A theoretical study on the adsorption of small molecules such as H_2, H_2O, N_2O and CO molecules on graphene and its doping derivatives with transition metals (Sc, Ti, Fe, Co, Ni, Zn and Au) using SCC-DFTB method at 298K. It was found that the highest adsorption of the H_2, H_2O, N_2O and CO are on the FeG, TiG, CoG and TiG, respectively. It was suggested that the FeG, TiG and CoG can be developed as H_2, CO and N_2O storage materials and the TiG can be used as desiccating material for adsorption of water in the system without CO.

Based on electrical conductivity, the AuG and NiG can be developed as H_2 and H_2O sensors, respectively. The FeG can be developed as N_2O and CO sensors in systems without CO and N_2O, respectively.

REFERENCES

[1] N. Tit, K. Said, N.M. Mahmoud, S. Kouser, Z.H. Yamani, Ab-initio investigation of adsorption of CO and CO2 molecules on graphene: Role of intrinsic defects on gas sensing, Applied Surface Science, 394 (2017) 219-230.

[2] J. Ni, M. Quintana, S. Song, Adsorption of small gas molecules on transition metal (Fe, Ni and Co, Cu) doped graphene: A systematic DFT study, Physica E: Low-Dimensional Systems and Nanostructures, 116 (2020) 113768.

[3] D. Cortes-Arriagada, A. Mella, Performance of doped graphene nanoadsorbents with first-row transition metals (ScZn) for the adsorption of water-soluble trivalent arsenicals: A DFT study, Journal of Molecular Liquids, 294 (2019) 111665.

[4] X. Jia, H. Zhang, Z. Zhang, L. An, First-principles investigation of vacancy-defected graphene and Mn-doped graphene towards adsorption of H2 S, Superlattices and Microstructures, 134 (2019) 106235.

[5] I.N. Levine, D.H. Busch, H. Shull, Quantum chemistry, Pearson Prentice Hall Upper Saddle River, NJ2009.

[6] W. Thiel, Semiempirical quantum–chemical methods, Wiley Interdisciplinary Reviews: Computational Molecular Science, 4 (2014) 145-157.

[7] J. Xu, P.M. Huang, Molecular environmental soil science at the interfaces in the earth's critical zone, Springer2010.

[8] M. Elstner, D. Porezag, G. Jungnickel, J. Elsner, M. Haugk, T. Frauenheim, S. Suhai, G. Seifert, Self-consistent-charge density-functional tight-binding method for simulations of complex materials properties, Physical Review B, 58 (1998) 7260.

[9] T.A. Niehaus, S. Suhai, F. Della Sala, P. Lugli, M. Elstner, G. Seifert, T. Frauenheim, Tight-binding approach to time-dependent density-functional response theory, Physical Review B, 63 (2001) 085108.

[10] H. Liu, M. Elstner, E. Kaxiras, T. Frauenheim, J. Hermans, W. Yang, Quantum mechanics simulation of protein dynamics on long timescale, Proteins: Structure, Function, and Bioinformatics, 44 (2001) 484-489.

[11] M.A. Marques, N.T. Maitra, F.M. Nogueira, E.K. Gross, A. Rubio, Fundamentals of time-dependent density functional theory, Springer Science & Business Media2012.

[12] M. Elstner, G. Seifert, Density functional tight binding, Philosophical Transactions of the Royal Society A: Mathematical, Physical and Engineering Sciences, 372 (2014) 20120483.

[13] B. Aradi, B. Hourahine, T. Frauenheim, DFTB+, a sparse matrix-based implementation of the DFTB method, The Journal of Physical Chemistry A, 111 (2007) 5678-5684.

APPENDIX

The binding energies of transition metal on single-vacancy defected in graphene using SCC-DFTB method.

Table S1. The binding energies of transition metal on single-vacancy defected in graphene

Reaction	$\Delta E_{binding}$, eV	$\Delta E_{binding}$, kcal/mol
[Vc + G] + Sc → Sc-G	-5.70	-131.56
[Vc + G] + Ti → Ti-G	-14.09	-324.97
[Vc + G] + Fe → Fe-G	-9.49	-218.76
[Vc + G] + Co → Co-G	-9.52	-219.65
[Vc + G] + Ni → Ni-G	-5.90	-135.94
[Vc + G] + Zn → Zn-G	-3.00	-69.21
[Vc + G] + Au → Au-G	-1.67	-38.43

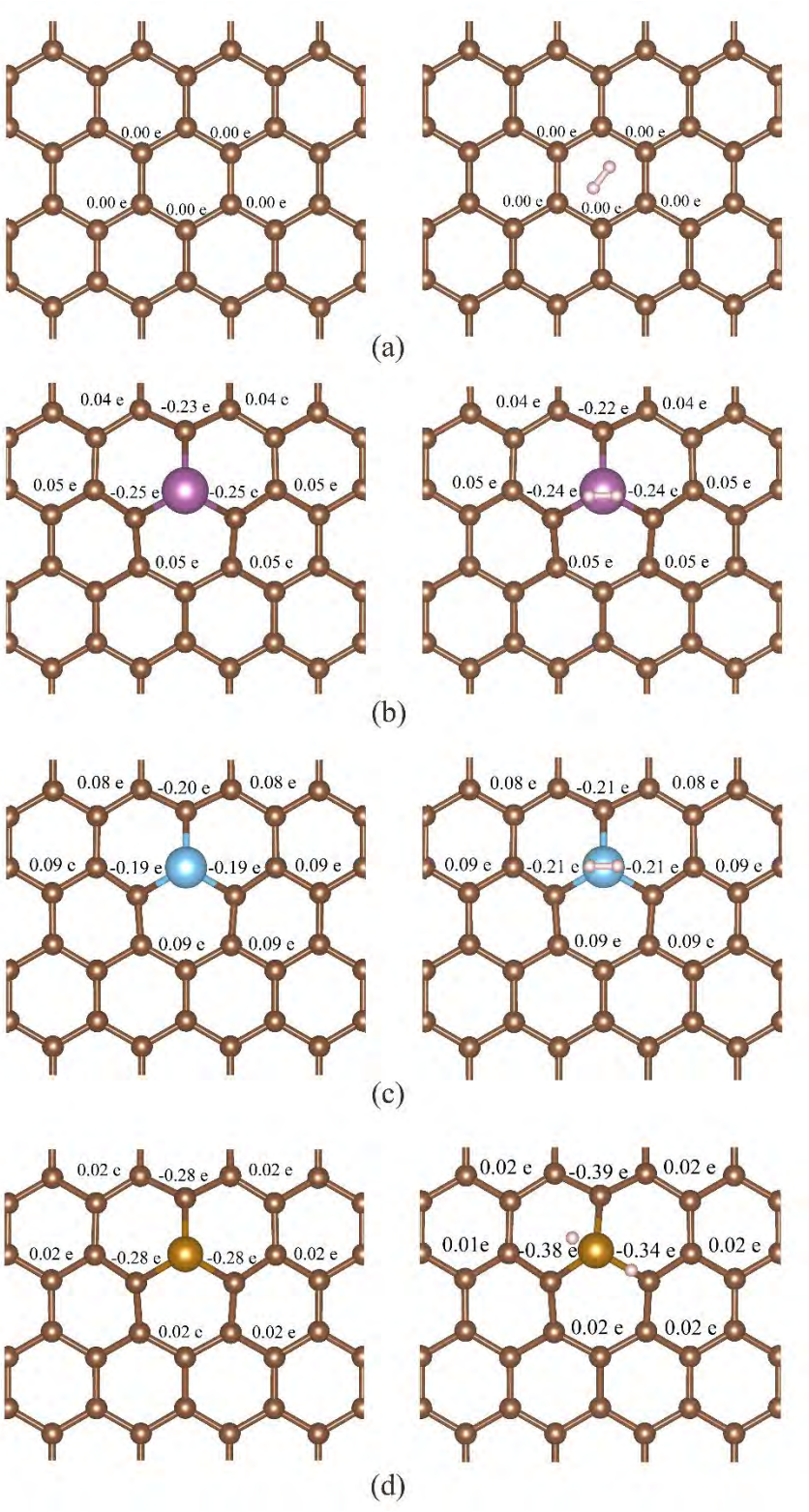

Figure S1. Mülliken charges of related atoms on (a) pristine, (b) Sc-doped G, (c) Ti-doped G and (d) Fe-doped G. Left and right views are clean and hydrogen molecule adsorbed surfaces.

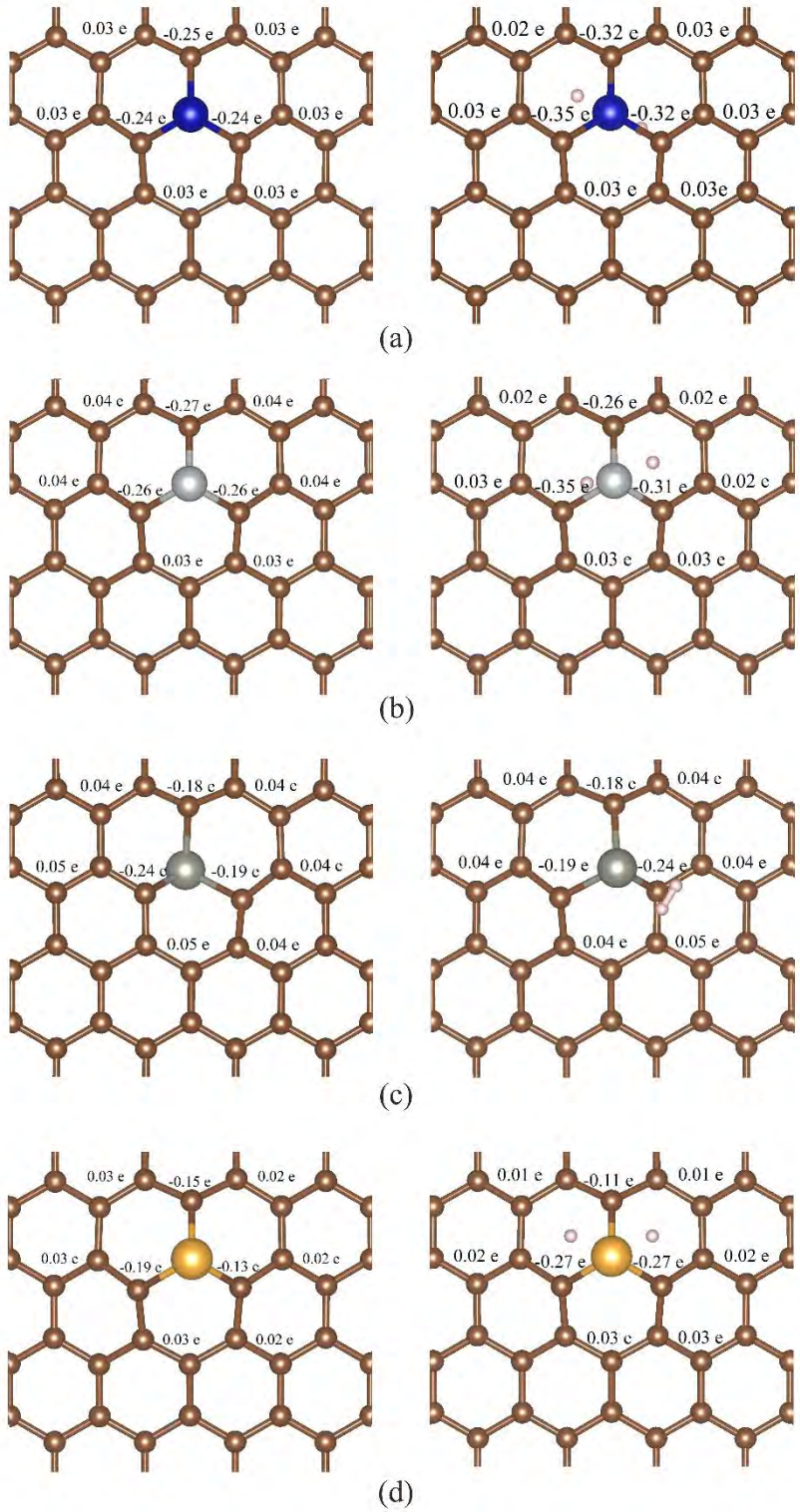

Figure S2. Mülliken charges of related atoms on (a) Co-doped, (b) Ni-doped G, (c) Zn-doped and (d) Au-doped G. Left and right views are clean and hydrogen molecule adsorbed surfaces.

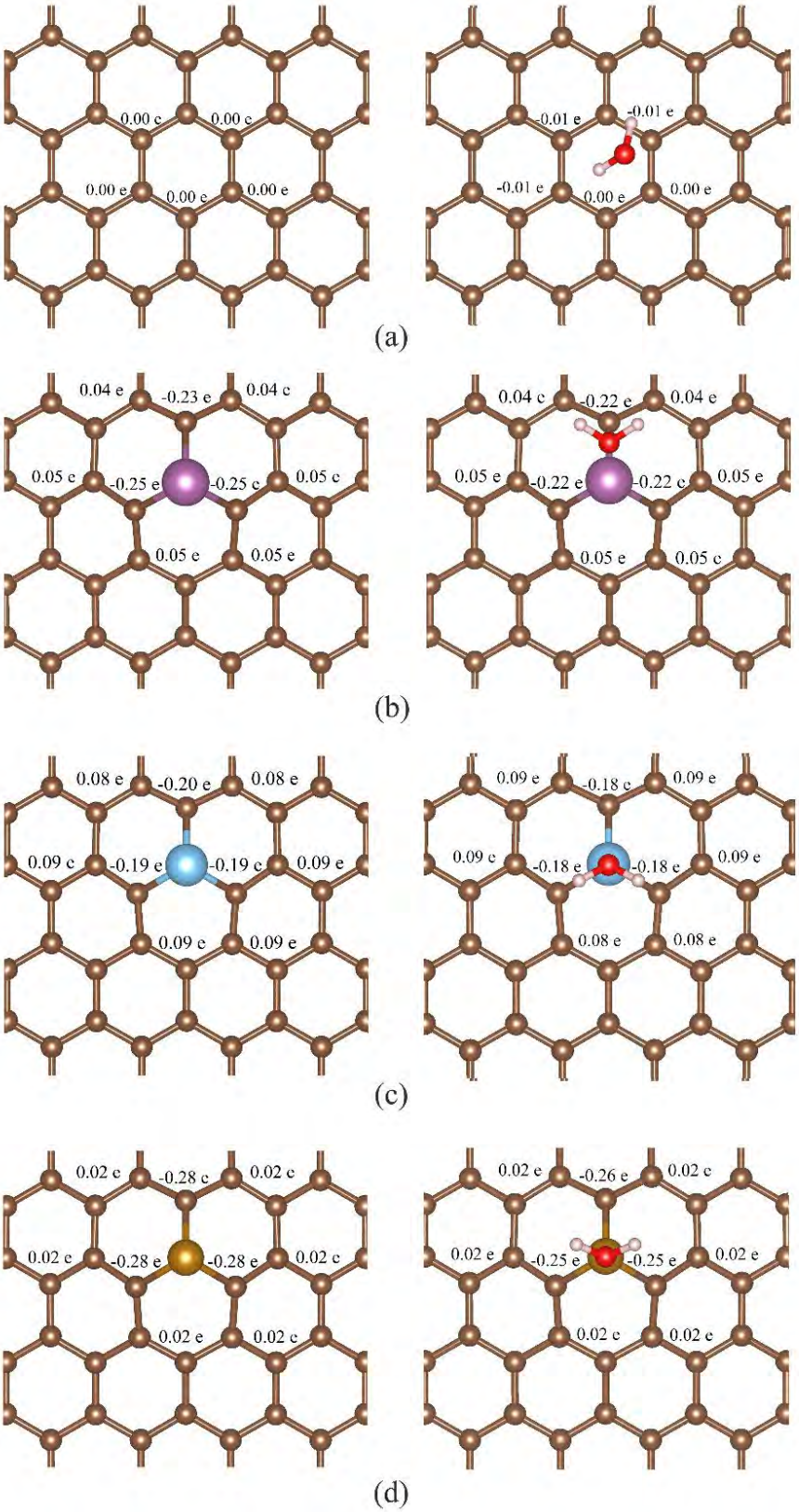

Figure S3. Mülliken charges of related atoms on (a) pristine, (b) Sc-doped G, (c) Ti-doped G and (d) Fe-doped G. Left and right views are clean and H_2O molecule adsorbed surfaces.

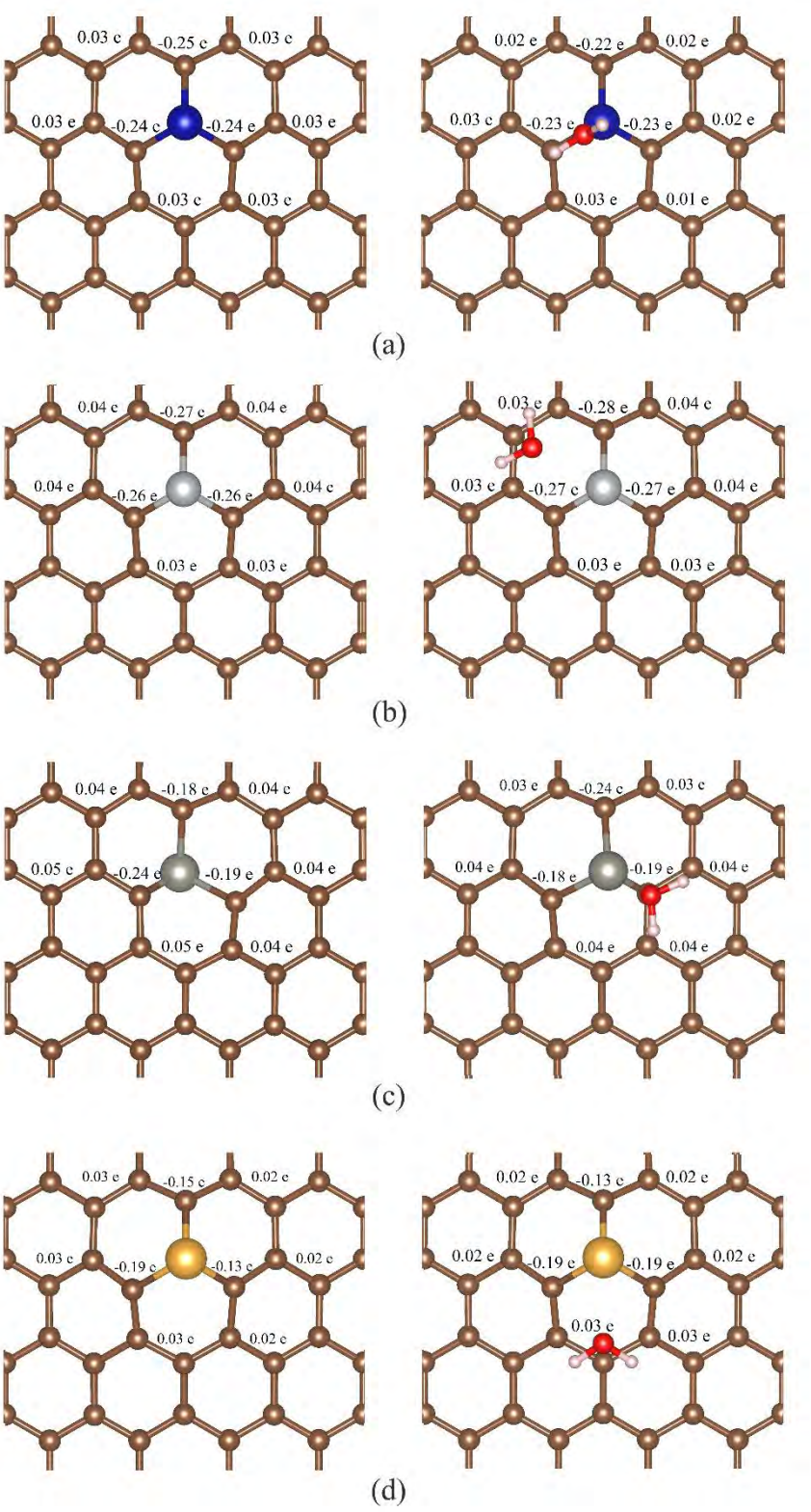

Figure S4. Mülliken charges of related atoms on (a) Co-doped, (b) Ni-doped G, (c) Zn-doped and (d) Au-doped G. Left and right views are clean and H_2O molecule adsorbed surfaces.

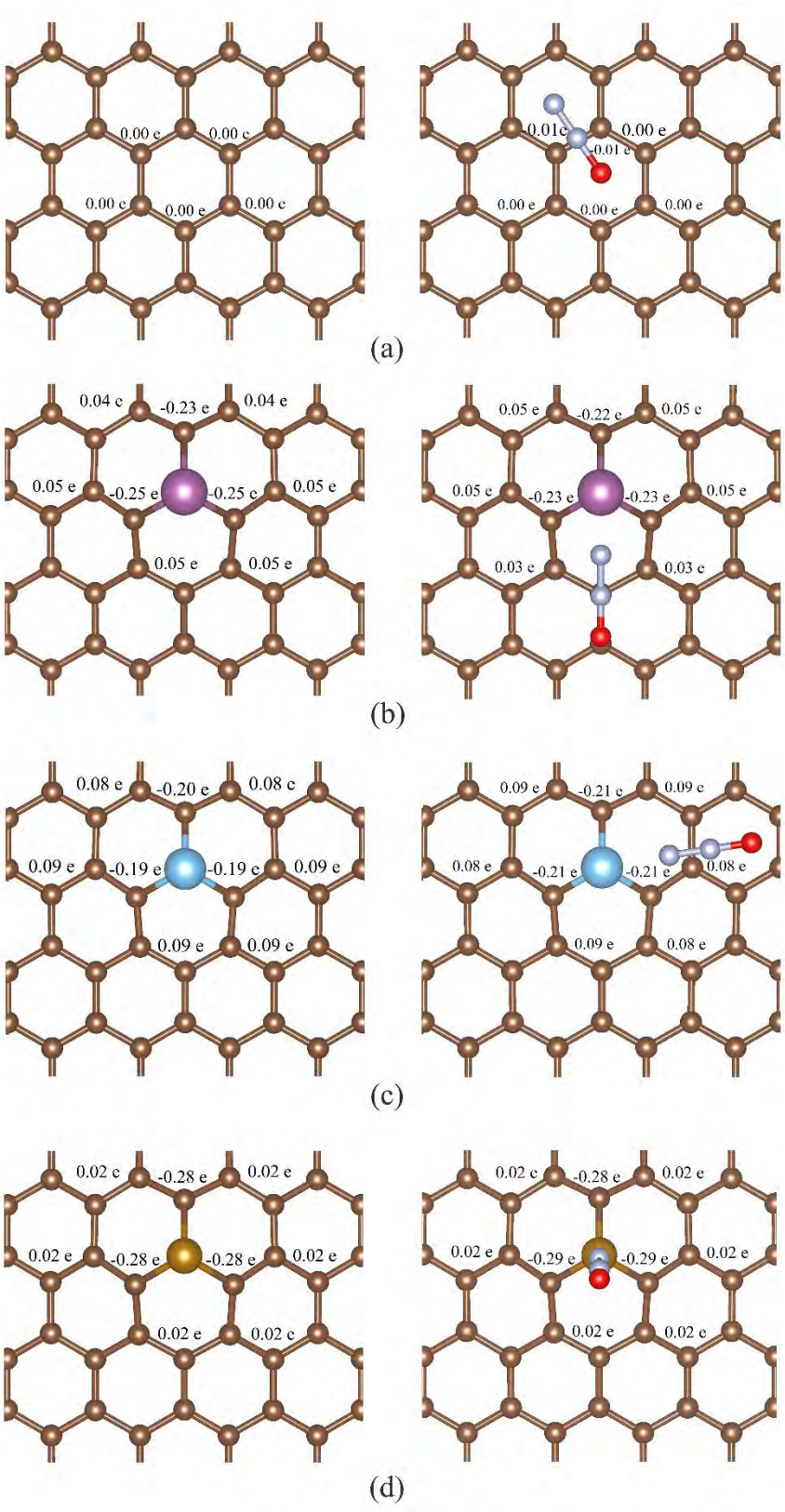

Figure S5. Mülliken charges of related atoms on (a) pristine, (b) Sc-doped G, (c) Ti-doped G and (d) Fe-doped G. Left and right views are clean and N_2O molecule as [M···N=N=O] adsorbed surfaces.

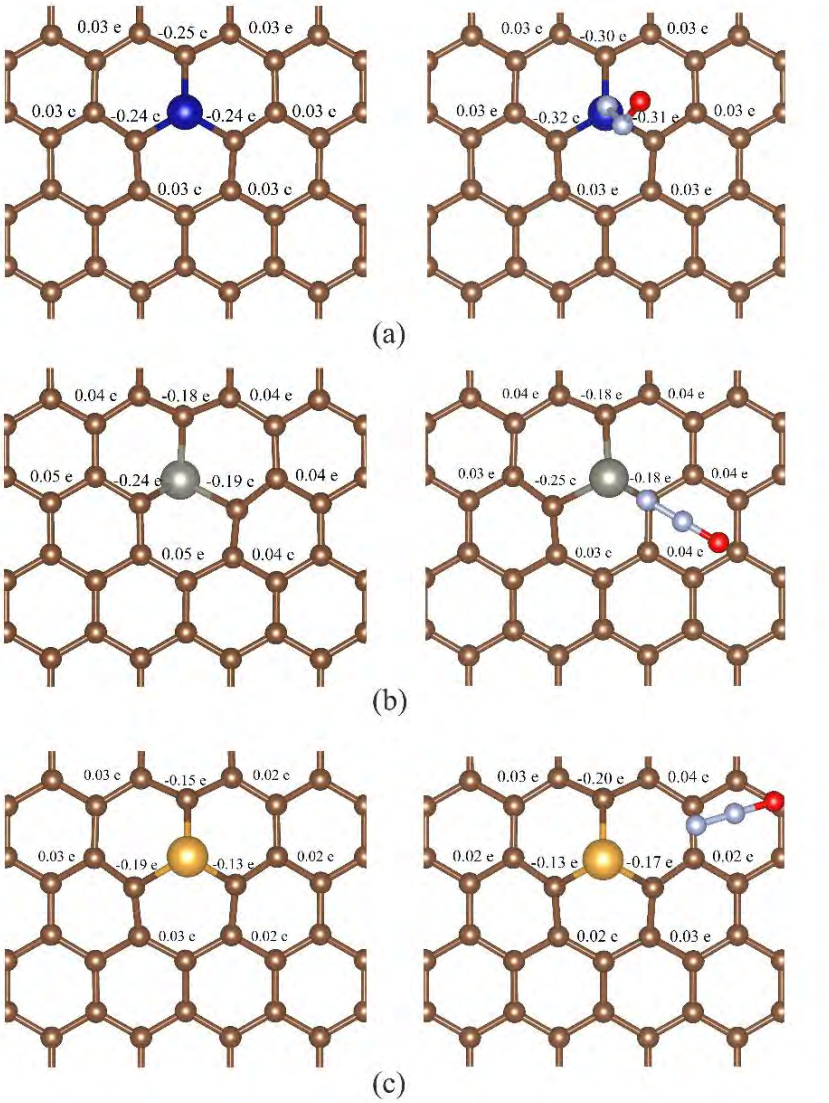

Figure S6. Mülliken charges of related atoms on (a) Co-doped, (b) Zn-doped and (c) Au-doped G. Left and right views are clean and N_2O molecule as [M···N=N=O] adsorbed surfaces.

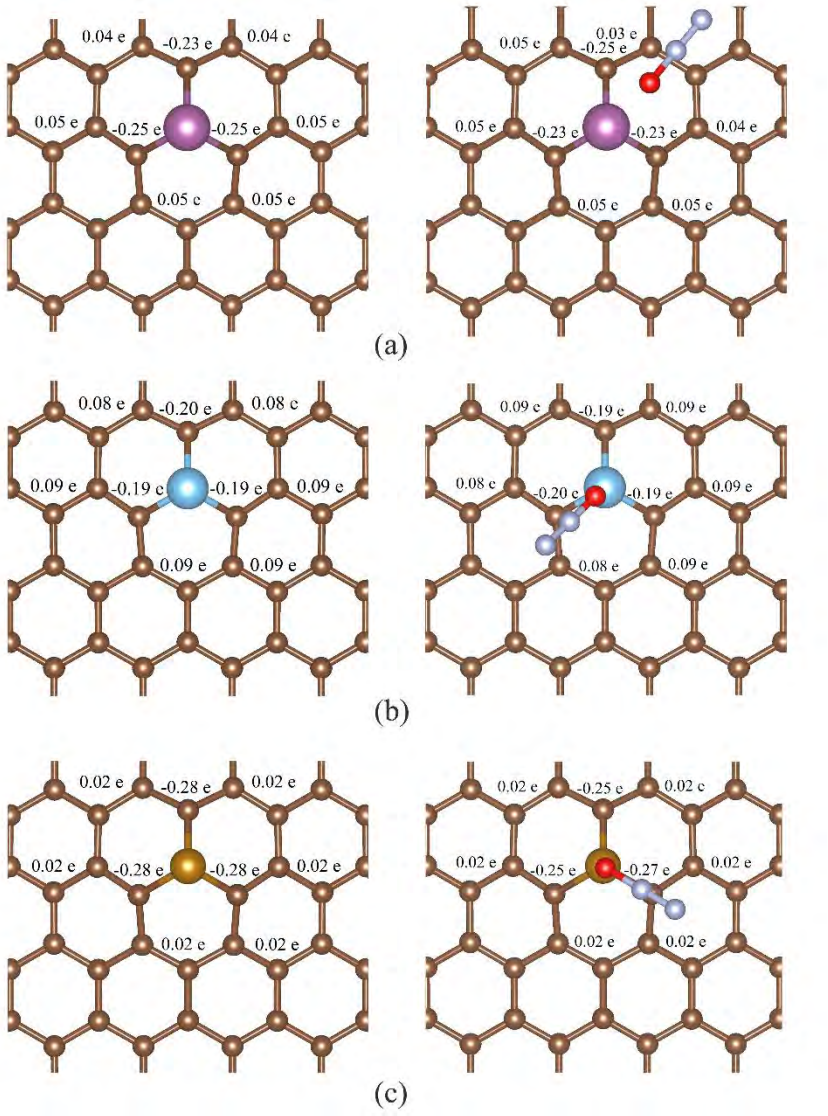

Figure S7. Mülliken charges of related atoms on (a) Sc-doped G, (b) Ti-doped G and (c) Fe-doped G. Left and right views are clean and N_2O molecule as [M···O=N=N] adsorbed surfaces.

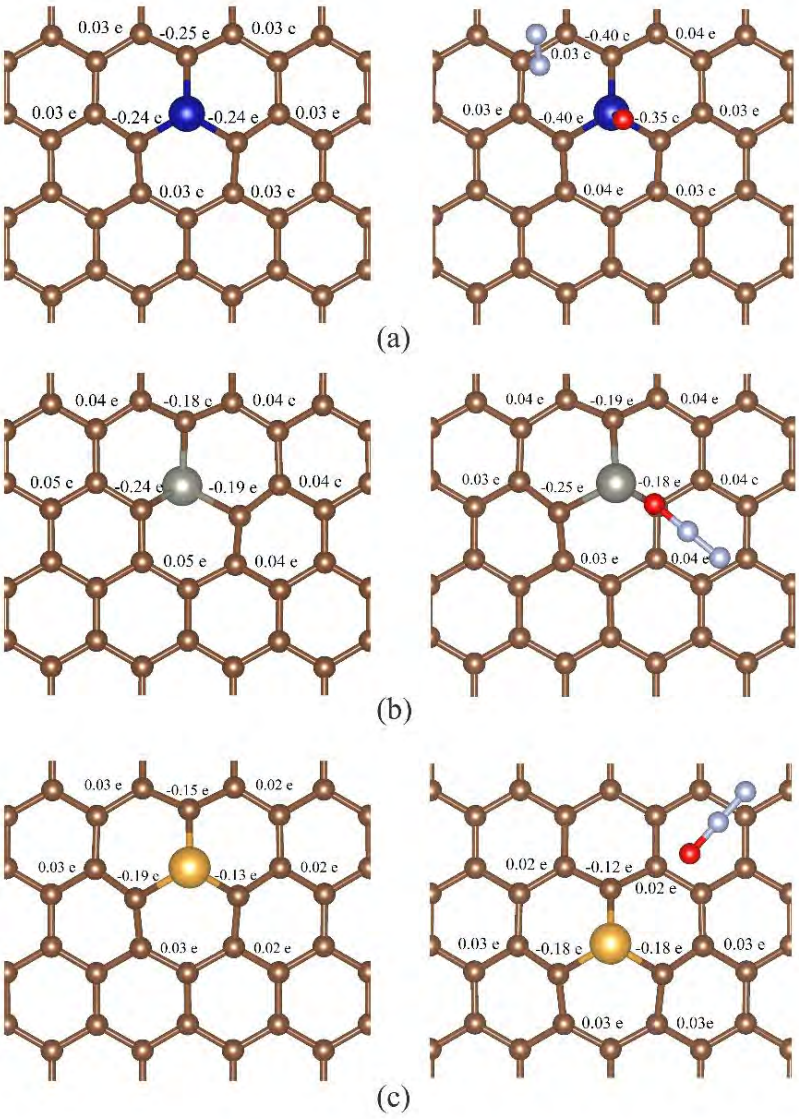

Figure S8. Mülliken charges of related atoms on (a) Co-doped G, (b) Zn-doped G and (c) Au-doped G. Left and right views are clean and N_2O molecule as [M···O=N=N] adsorbed surfaces.

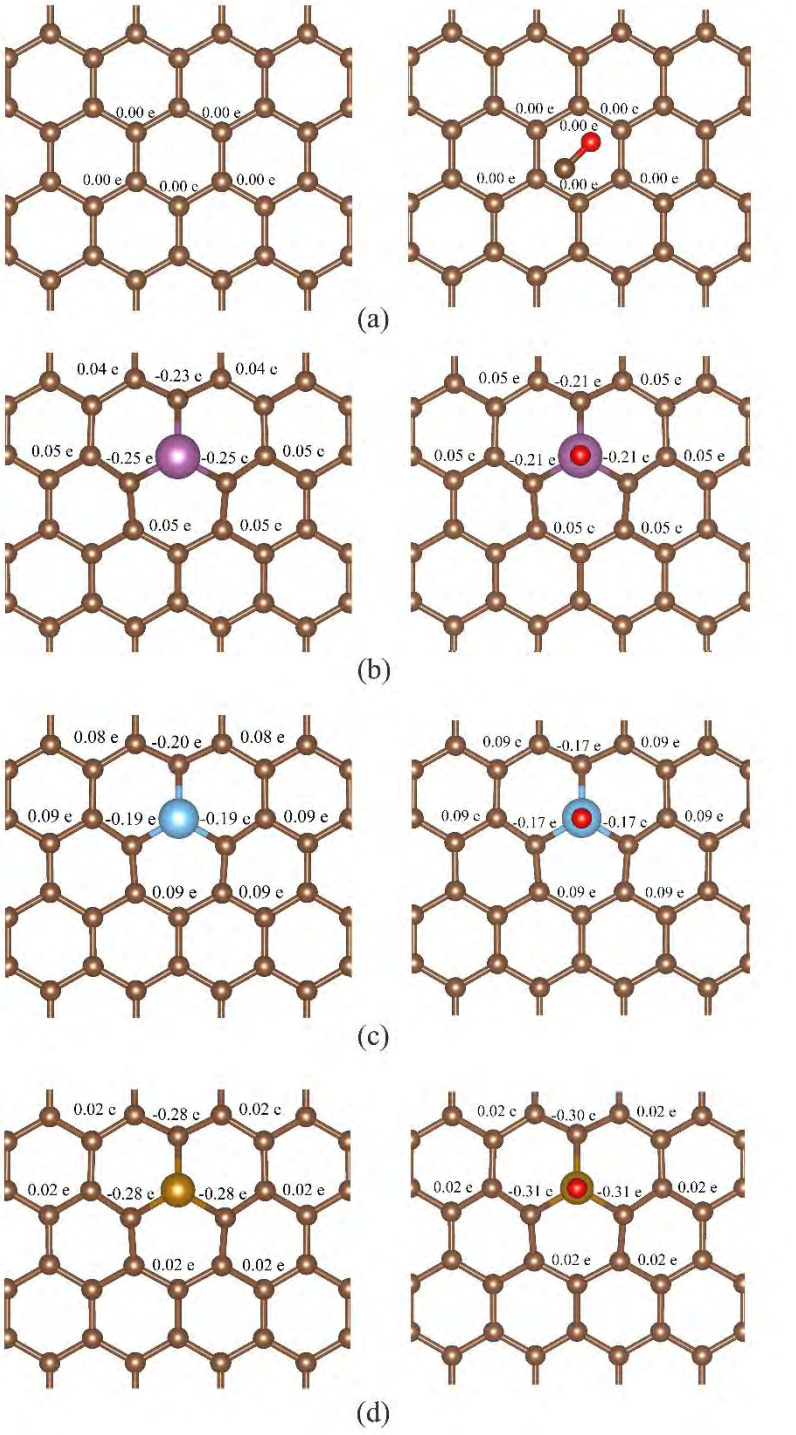

Figure S9. Mülliken charges of related atoms on (a) pristine, (b) Sc-doped G, (c) Ti-doped G and (d) Fe-doped G. Left and right views are clean and CO molecule as [M· · ·C=O] adsorbed surfaces.

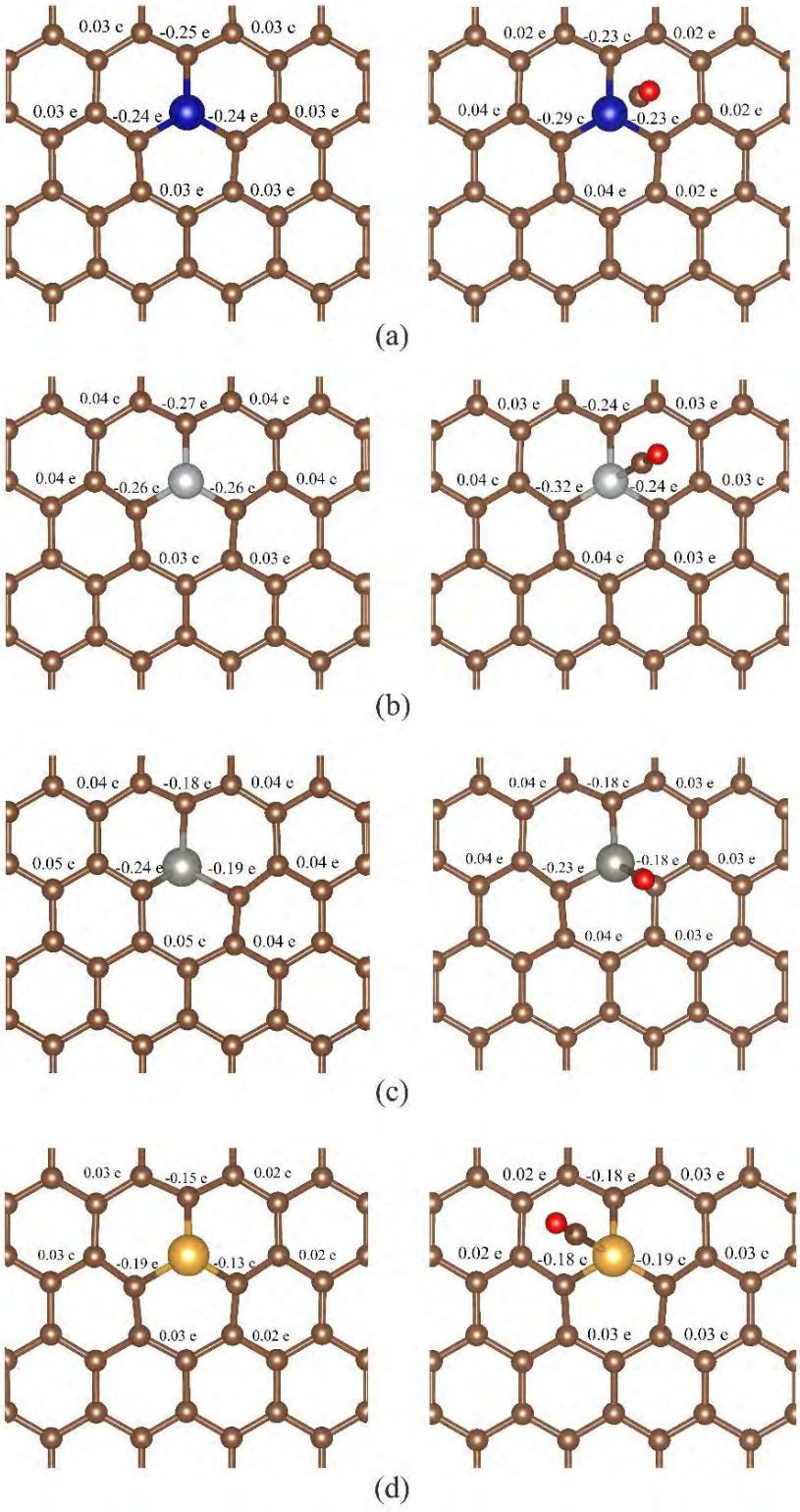

Figure S10. Mülliken charges of related atoms on (a) Co-doped, (b) Ni-doped G, (c) Zn-doped G and (d) Au-doped G. Left and right views are clean and CO molecule as [M· · ·C=O] adsorbed surfaces.

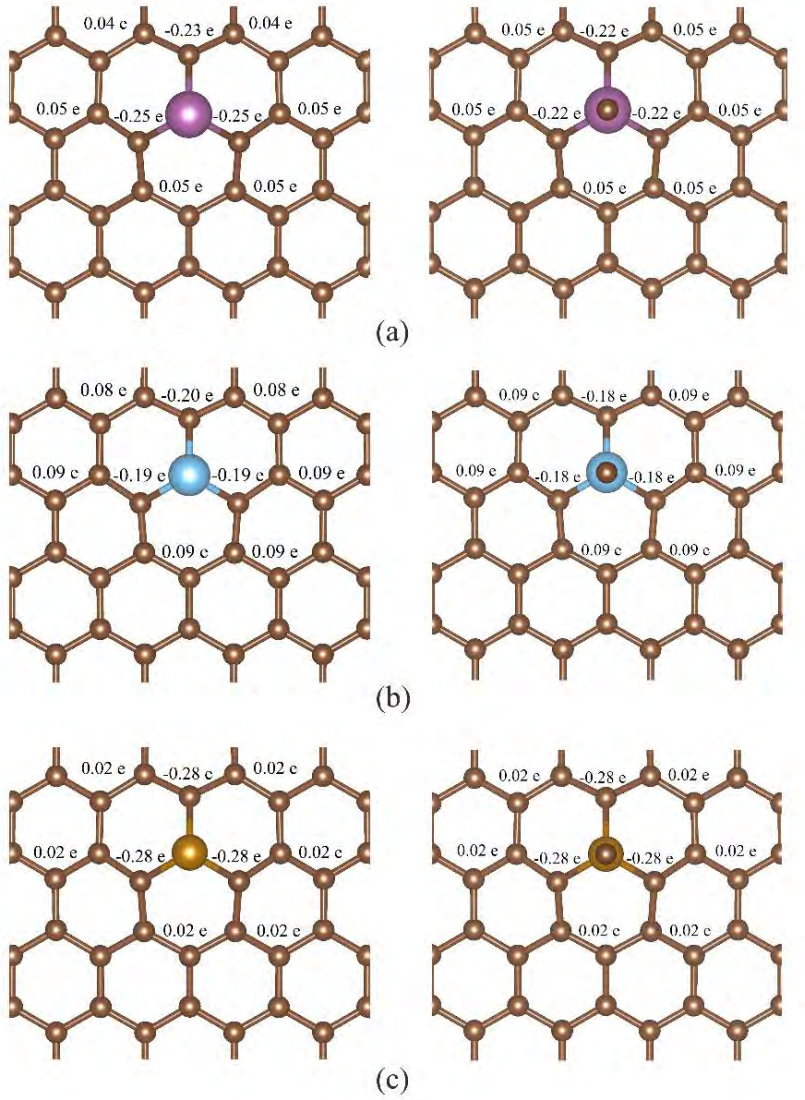

Figure S11. Mülliken charges of related atoms on (a) Sc-doped G, (b) Ti-doped G and (c) Fe-doped G. Left and right views are clean and CO molecule as [M· · ·O=C] adsorbed surfaces.

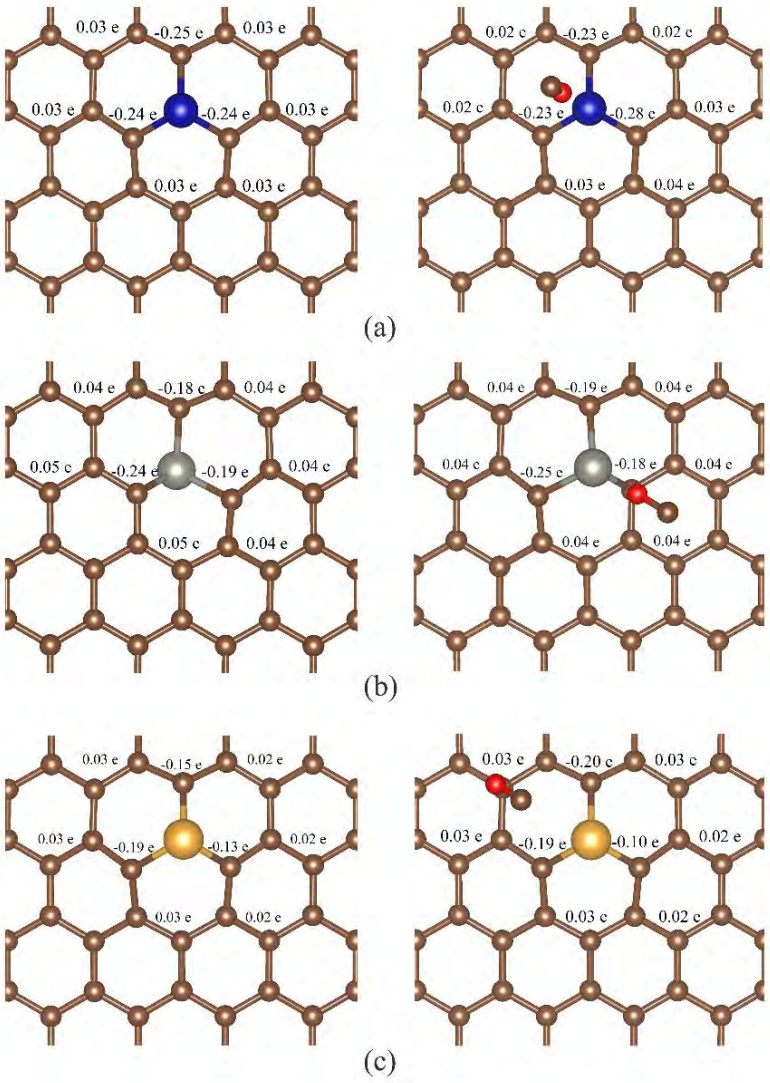

Figure S12. Mülliken charges of related atoms on (a) Co-doped, (b) Zn-doped G and (c) Au-doped G. Left and right views are clean and CO molecule as [M· · ·O=C] adsorbed surfaces.

VITAE

My name is Thitipong Sitthanaputtikorn. I was born on 11th July 1997. My address is 387/21 Donnok 11 Road, Suratthani 84000, Thailand. I graduated from high school at Suratthani School in 2016. I have studied in Bachelor's degree of Science, Chulalongkorn University during 2016 – 2019. My contact is thitipong.jj@gmail.com